APPENDIX C: CONSTRUCTION SIMULATION RESULTS

[This page is intentionally left blank]

Maximum SSC for the construction scenario of the 10-year ARI event

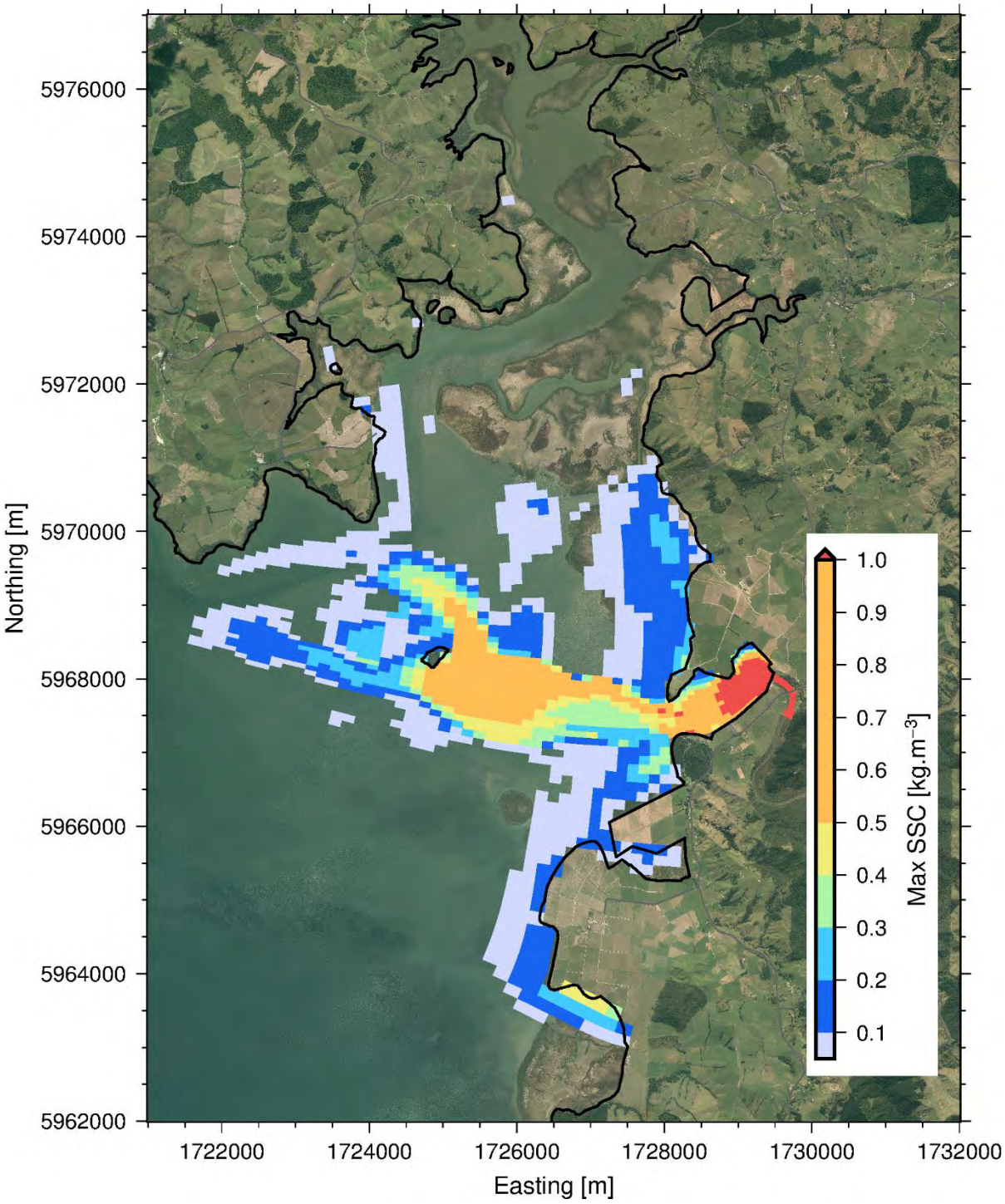

Figure 73: Maximum SSC for the construction scenario of the 10-year ARI, calm wind event. Note: Suspended sediment concentration below 0.005 kg/m^3 are not shown here.

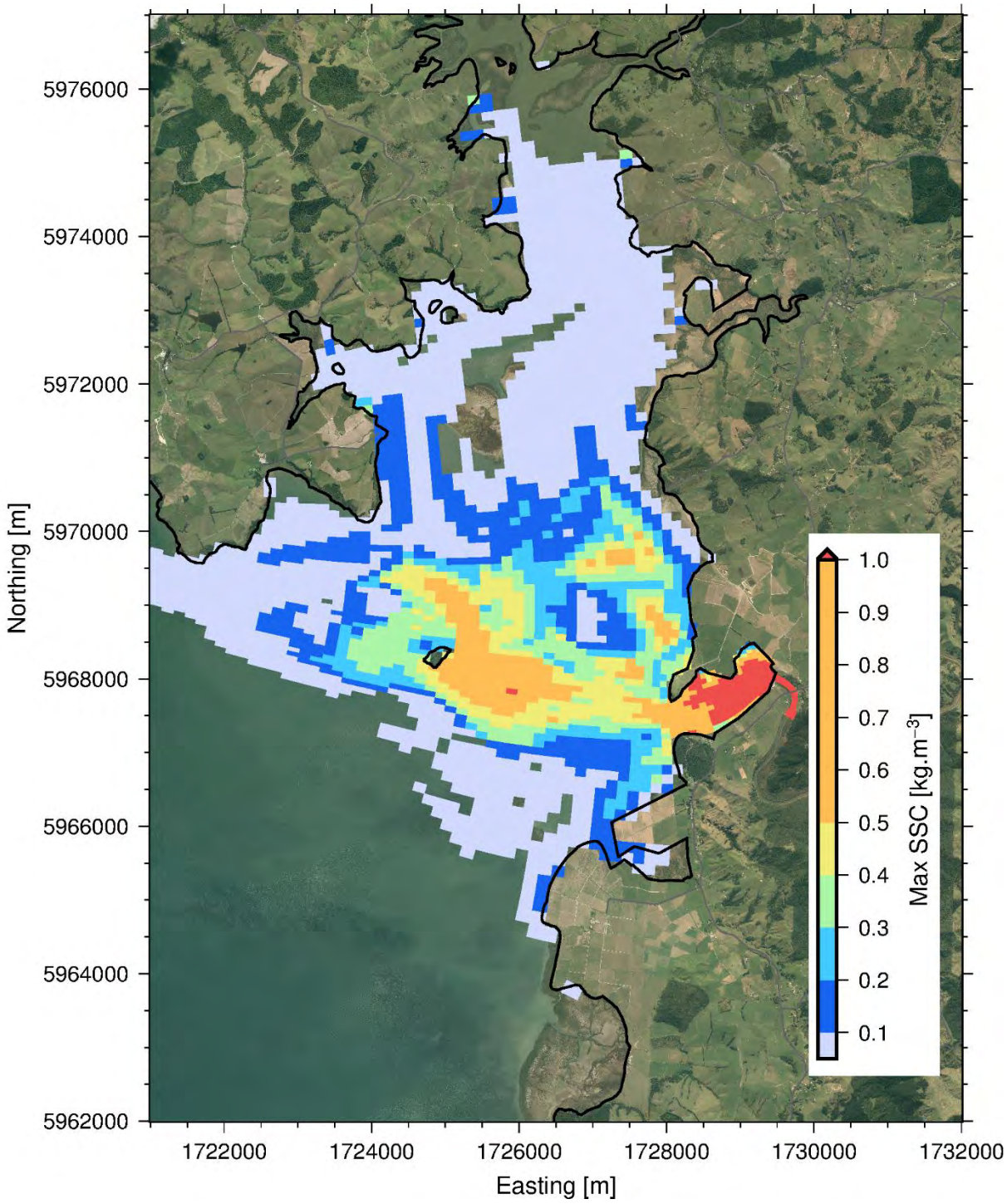

Figure 74: Maximum SSC for the construction scenario of the 10-year ARI, SW wind event. Note: Suspended sediment concentration below 0.005 kg/m^3 are not shown here.

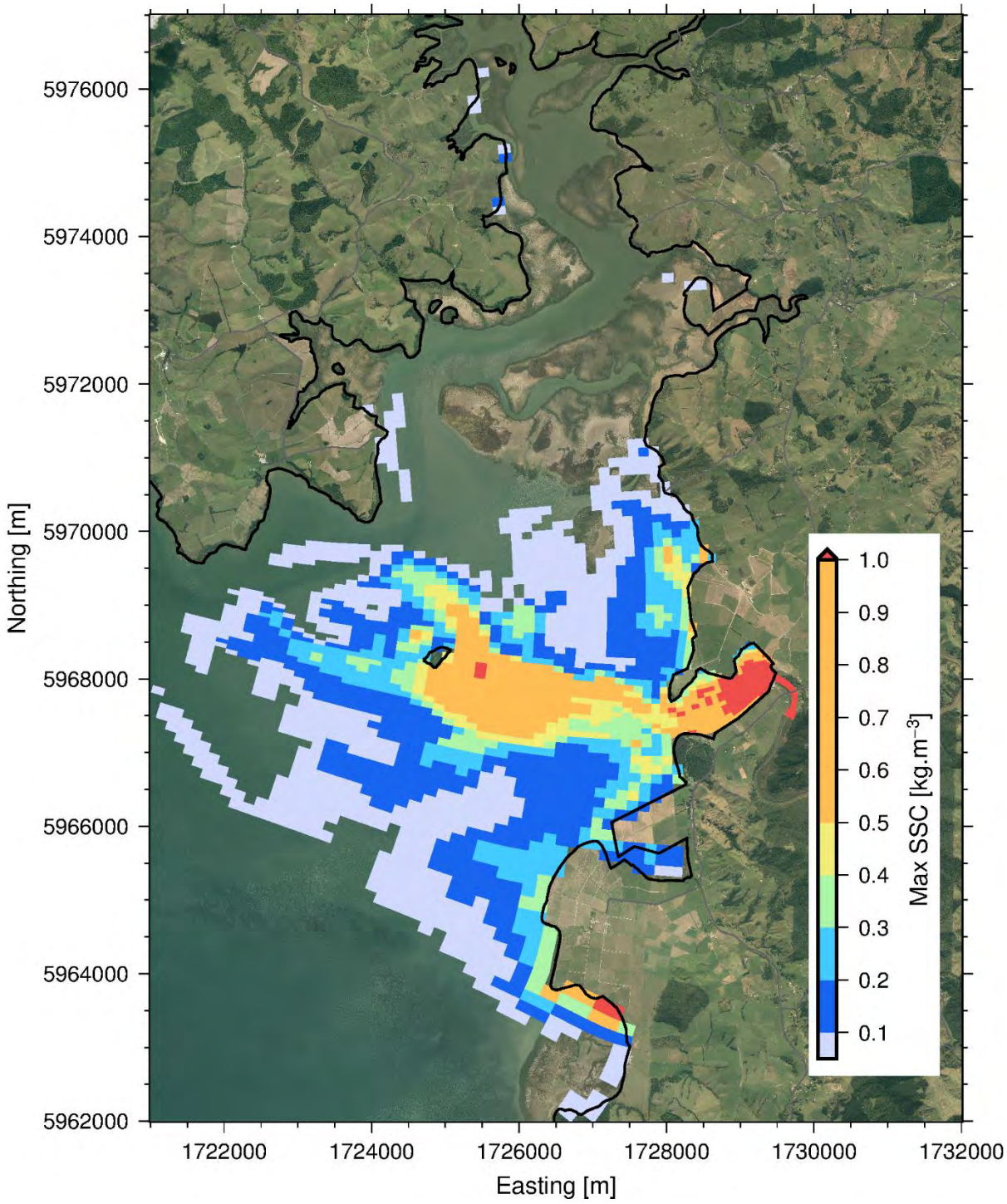

Figure 75: Maximum SSC for the construction scenario of the 10-year ARI, NE wind event. Note: Suspended sediment concentration below 0.005 kg/m^3 are not shown here.

Maximum SSC for the construction scenario of the 50-year ARI event

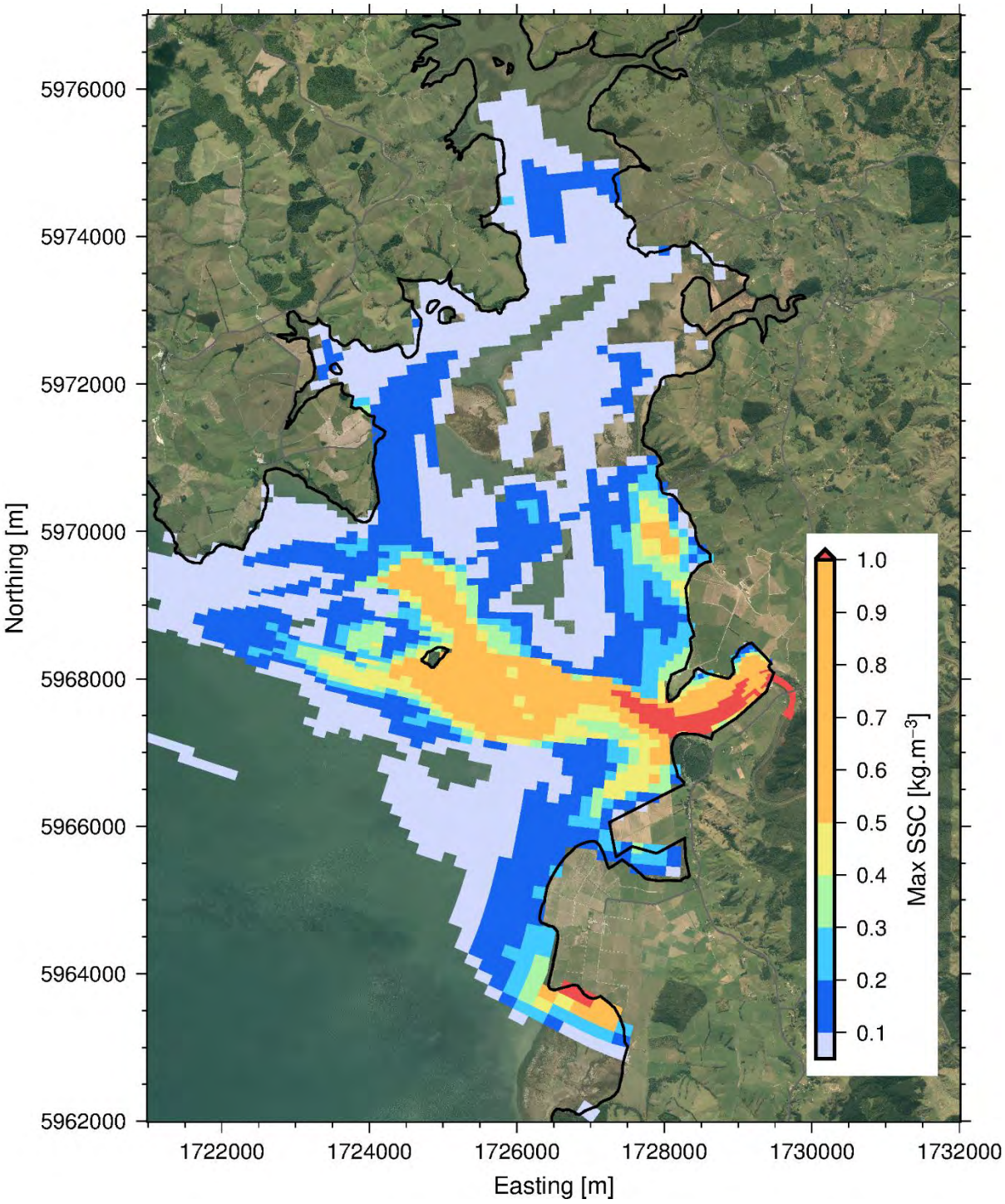

Figure 76: Maximum SSC for the construction scenario of the 50-year ARI, calm wind event. Note: Suspended sediment concentration below 0.005 kg/m^3 are not shown here.

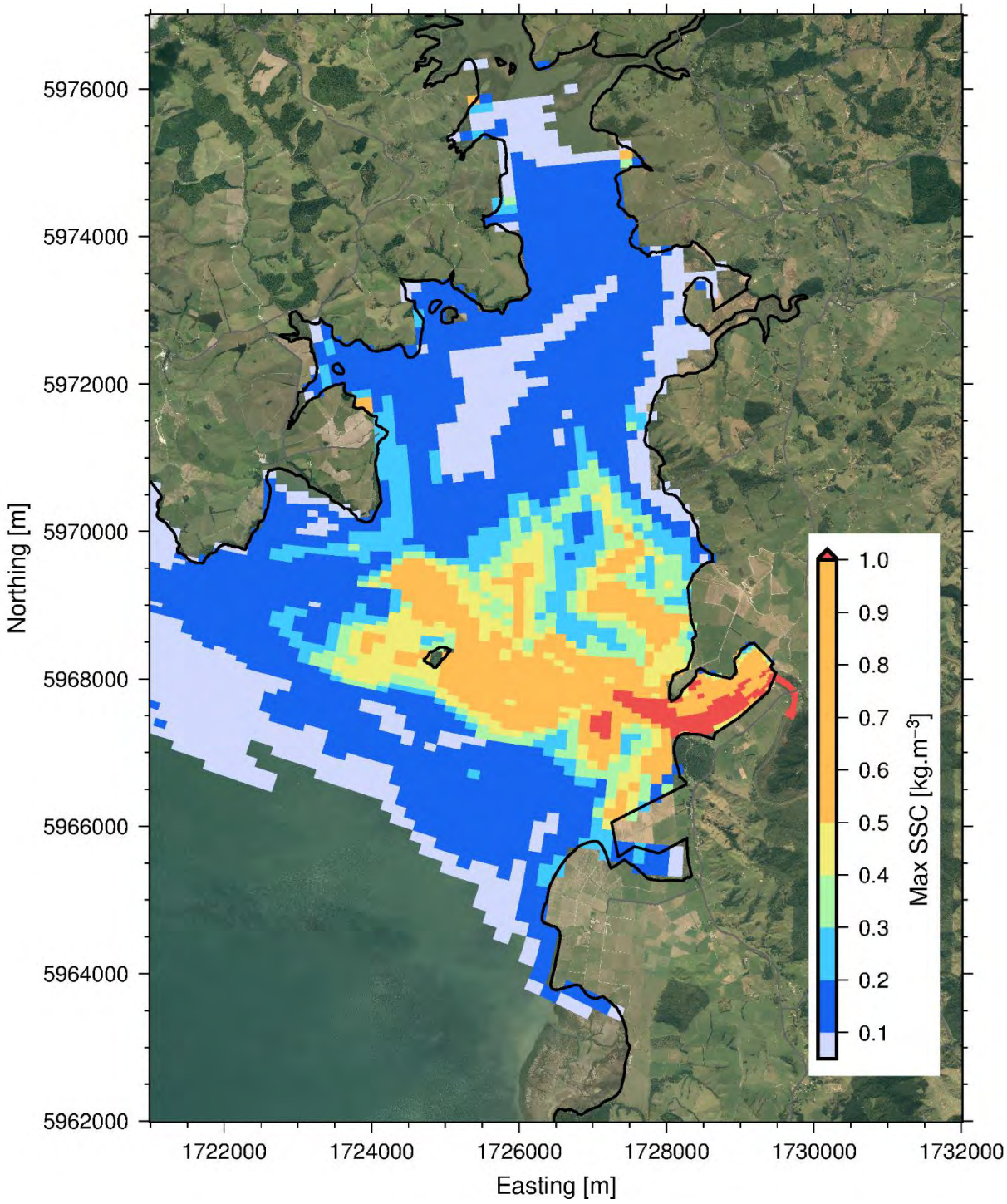

Figure 77: Maximum SSC for the construction scenario of the 50-year ARI, SW wind event. Note: Suspended sediment concentration below 0.005 kg/m^3 are not shown here.

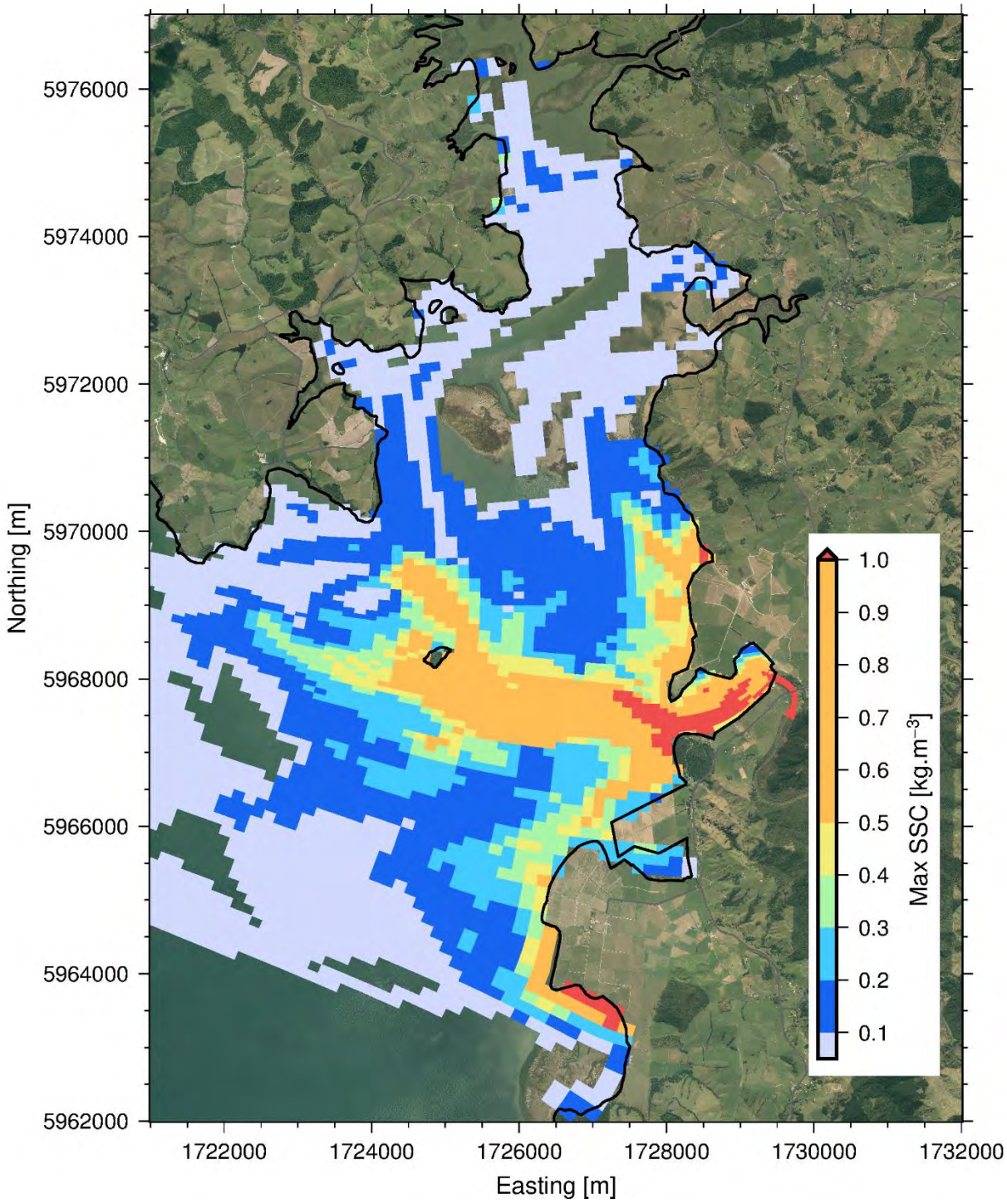

Figure 78: Maximum SSC for the construction scenario of the 50-year ARI, NE wind event. Note: Suspended sediment concentration below 0.005 kg/m^3 are not shown here.

Suspended sediment concentration 1 day after the start of the event for the construction 10-year ARI event

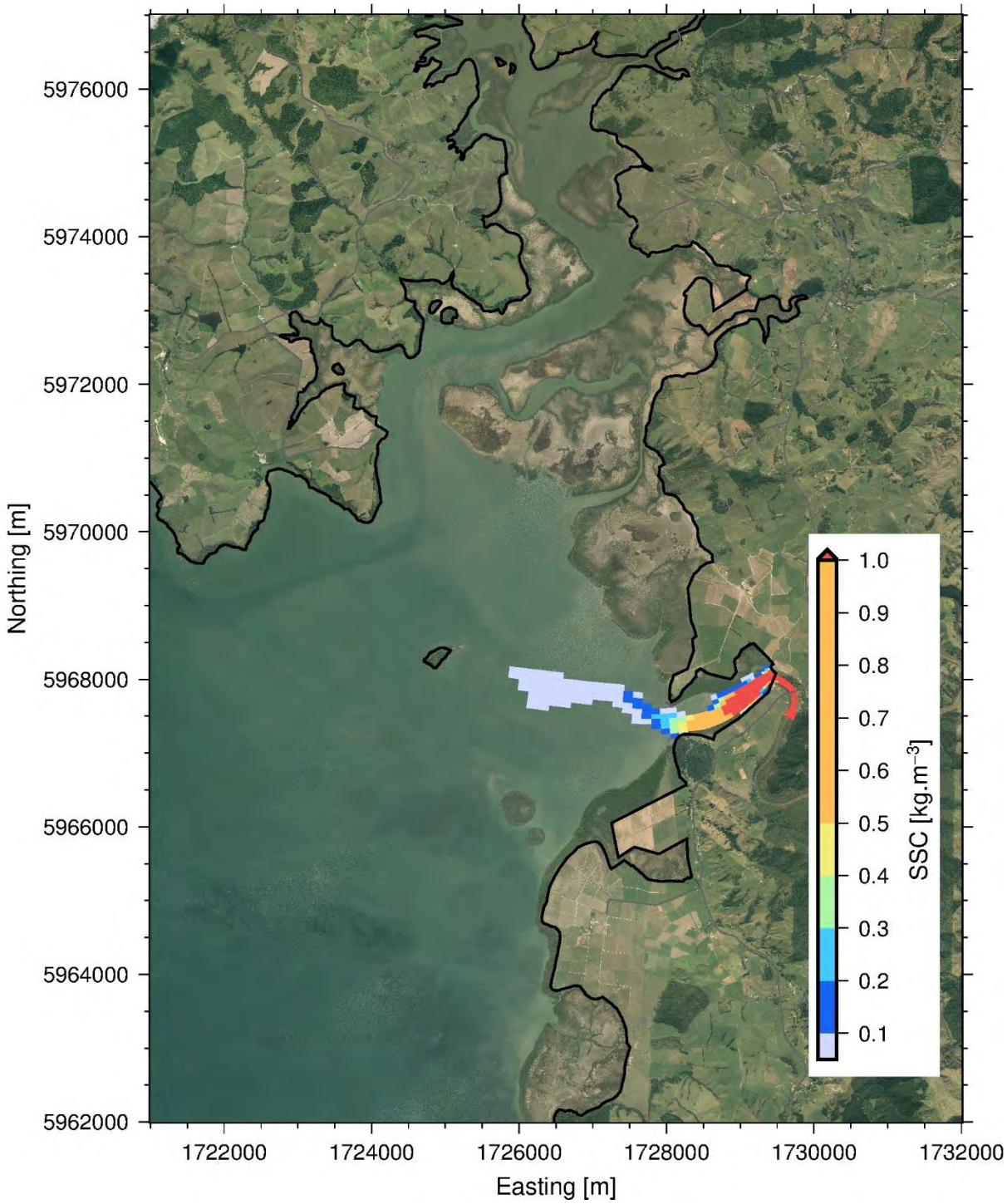

Figure 79: Suspended sediment concentration 1 day after the start of the event for the construction 10-year ARI, calm wind event. Note the start of the event is when the suspended sediment concentration exceeds 0.01 kg/m^3 in the model input.

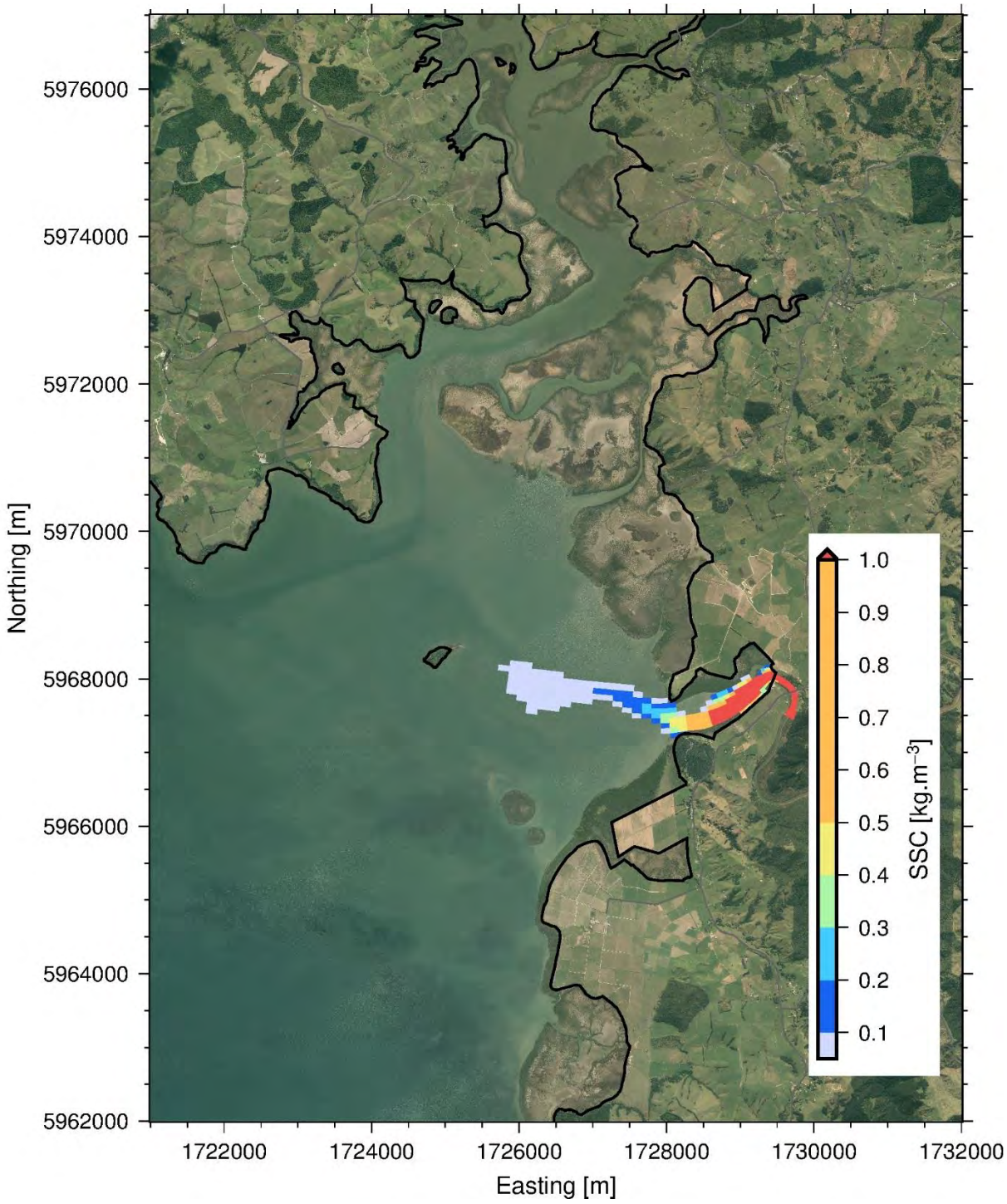

Figure 80: Suspended sediment concentration 1 day after the start of the event for the construction 10-year ARI, SW wind event. Note the start of the event is when the suspended sediment concentration exceeds 0.01 kg/m^3 in the model input.

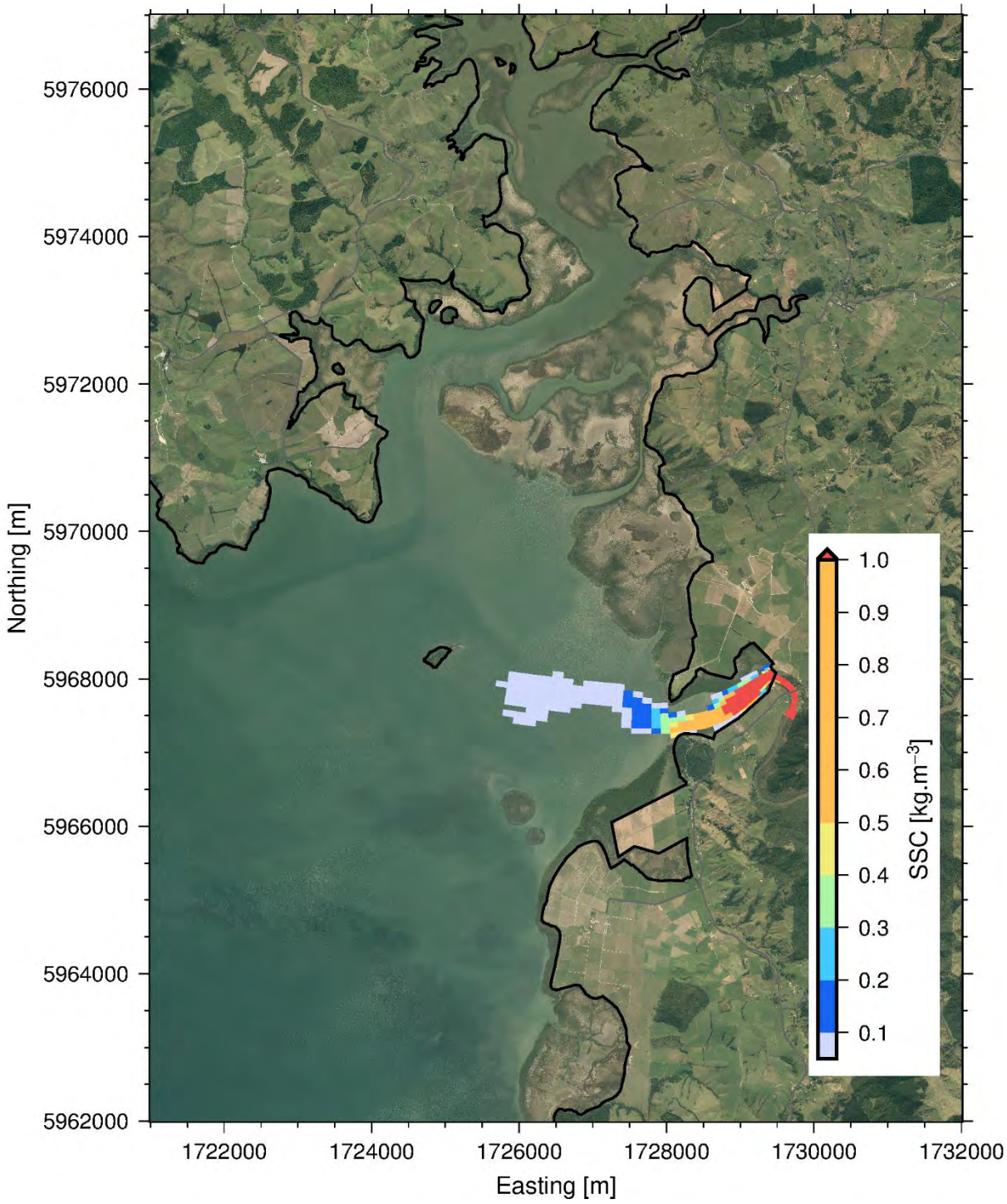

Figure 81: Suspended sediment concentration 1 day after the start of the event for the construction 10-year ARI, NE wind event. Note the start of the event is when the suspended sediment concentration exceeds 0.01 kg/m^3 in the model input.

Suspended sediment concentration 3 days after the start of the event for the construction 10-year ARI event

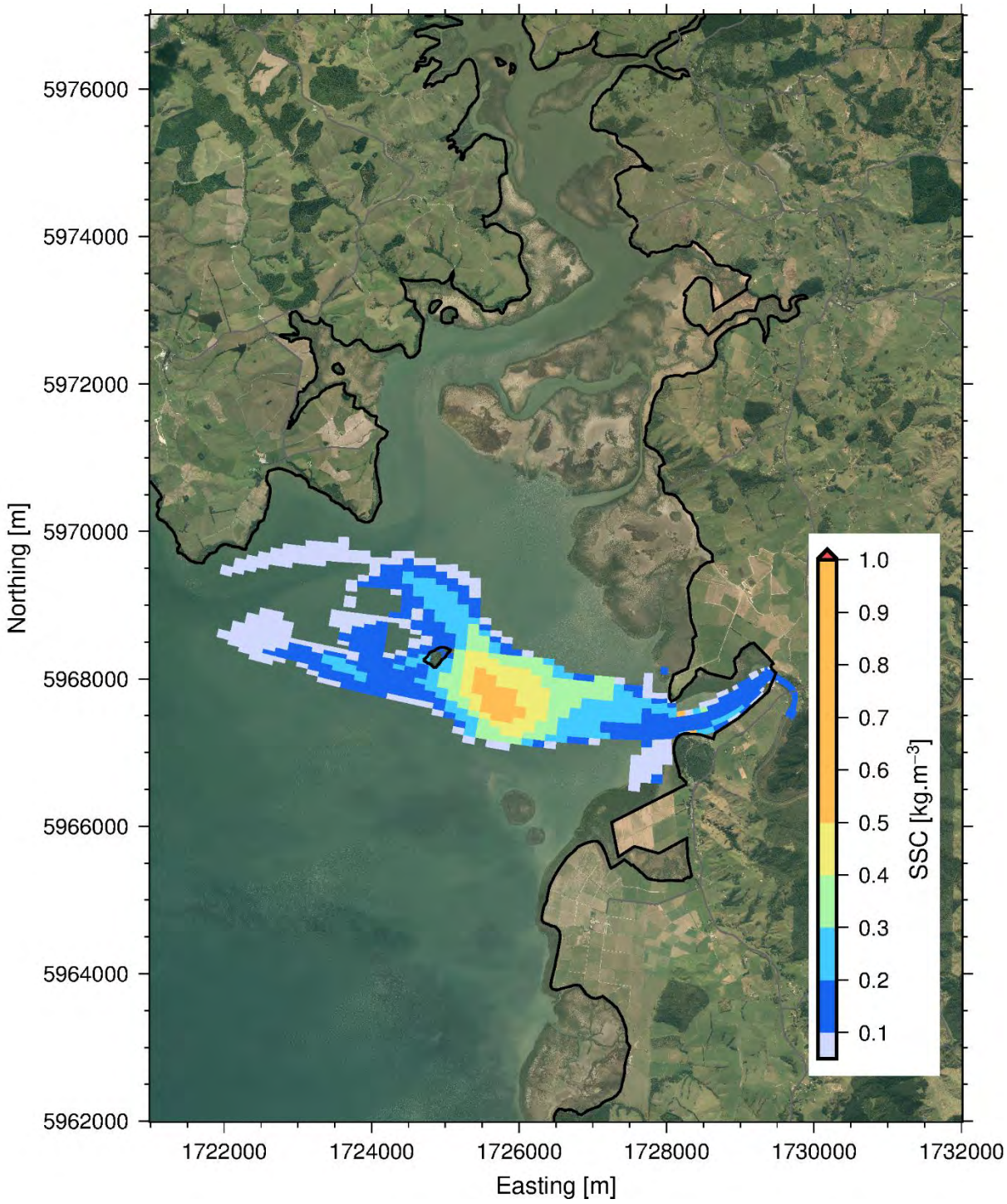

Figure 82: Suspended sediment concentration 3 days after the start of the event for the construction 10-year ARI, calm wind event. Note the start of the event is when the suspended sediment concentration exceeds 0.01 kg/m^3 in the model input.

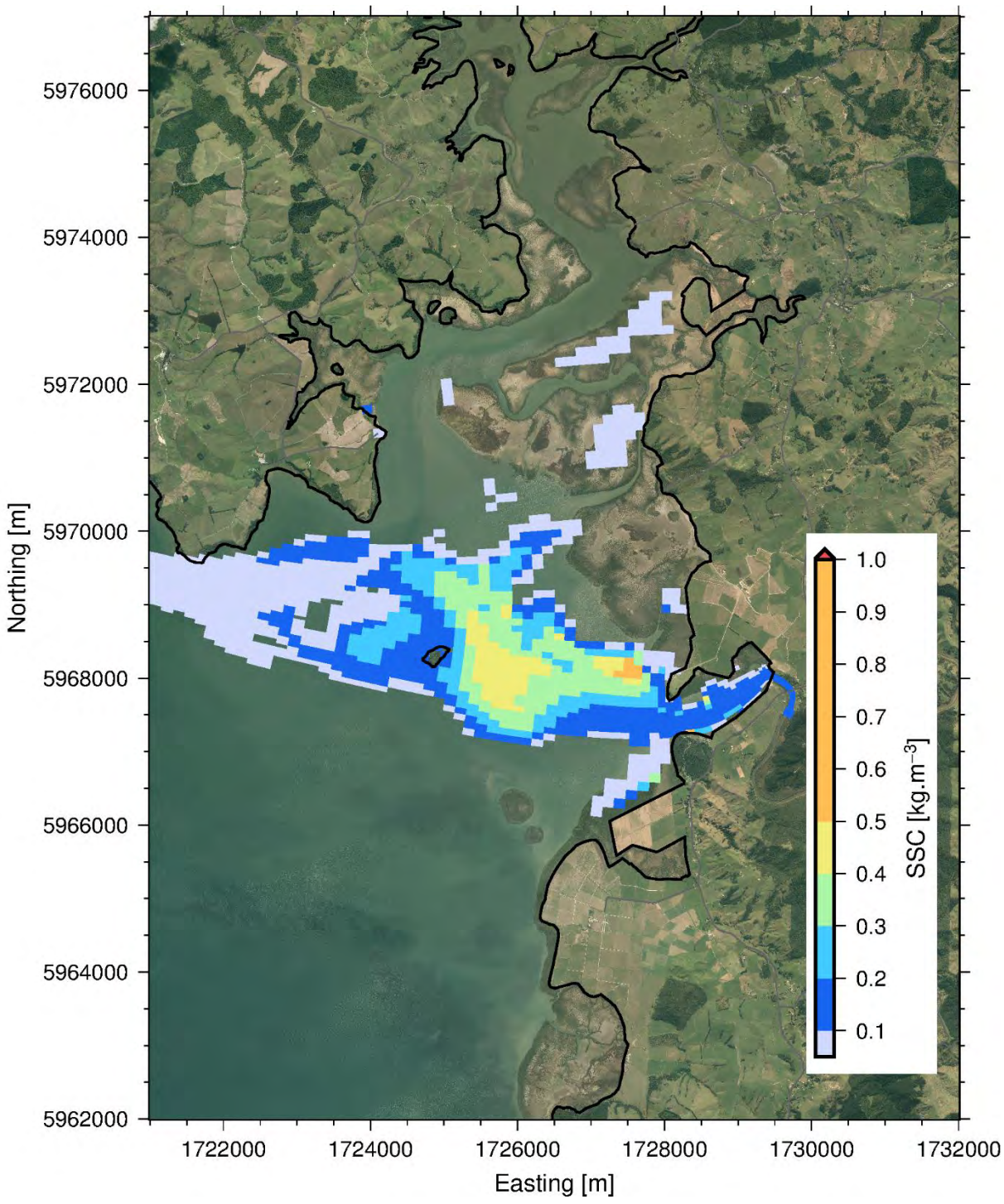

Figure 83: Suspended sediment concentration 3 days after the start of the event for the construction 10-year ARI, SW wind event. Note the start of the event is when the suspended sediment concentration exceeds 0.01 kg/m^3 in the model input.

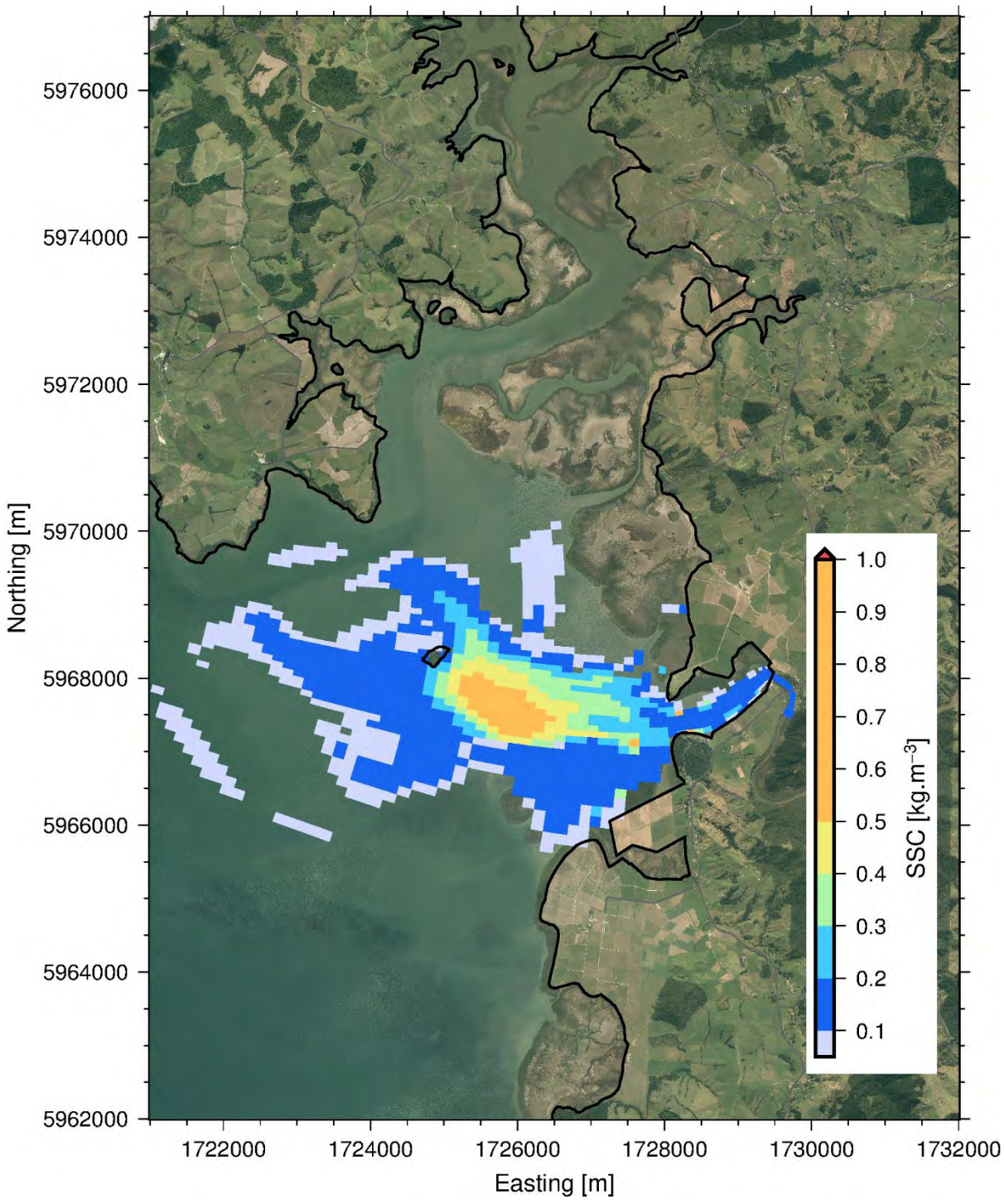

Figure 84: Suspended sediment concentration 3 days after the start of the event for the construction 10-year ARI, NE wind event. Note the start of the event is when the suspended sediment concentration exceeds 0.01 kg/m^3 in the model input.

Suspended sediment concentration 1 day after the start of the event for the construction 50-year ARI event

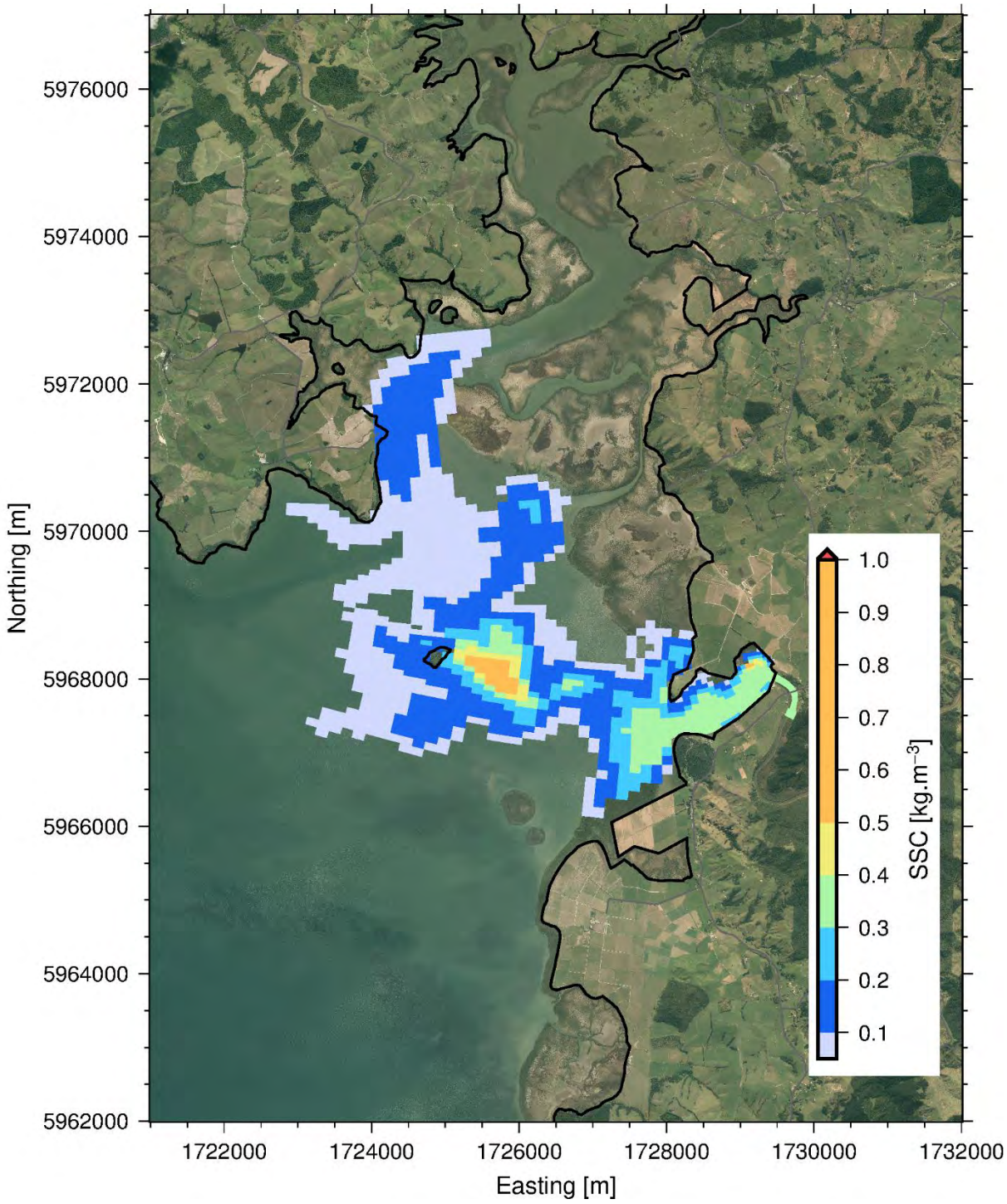

Figure 85: Suspended sediment concentration 1 day after the start of the event for the construction 50-year ARI, calm wind event. Note the start of the event is when the suspended sediment concentration exceeds 0.01 kg/m^3 in the model input.

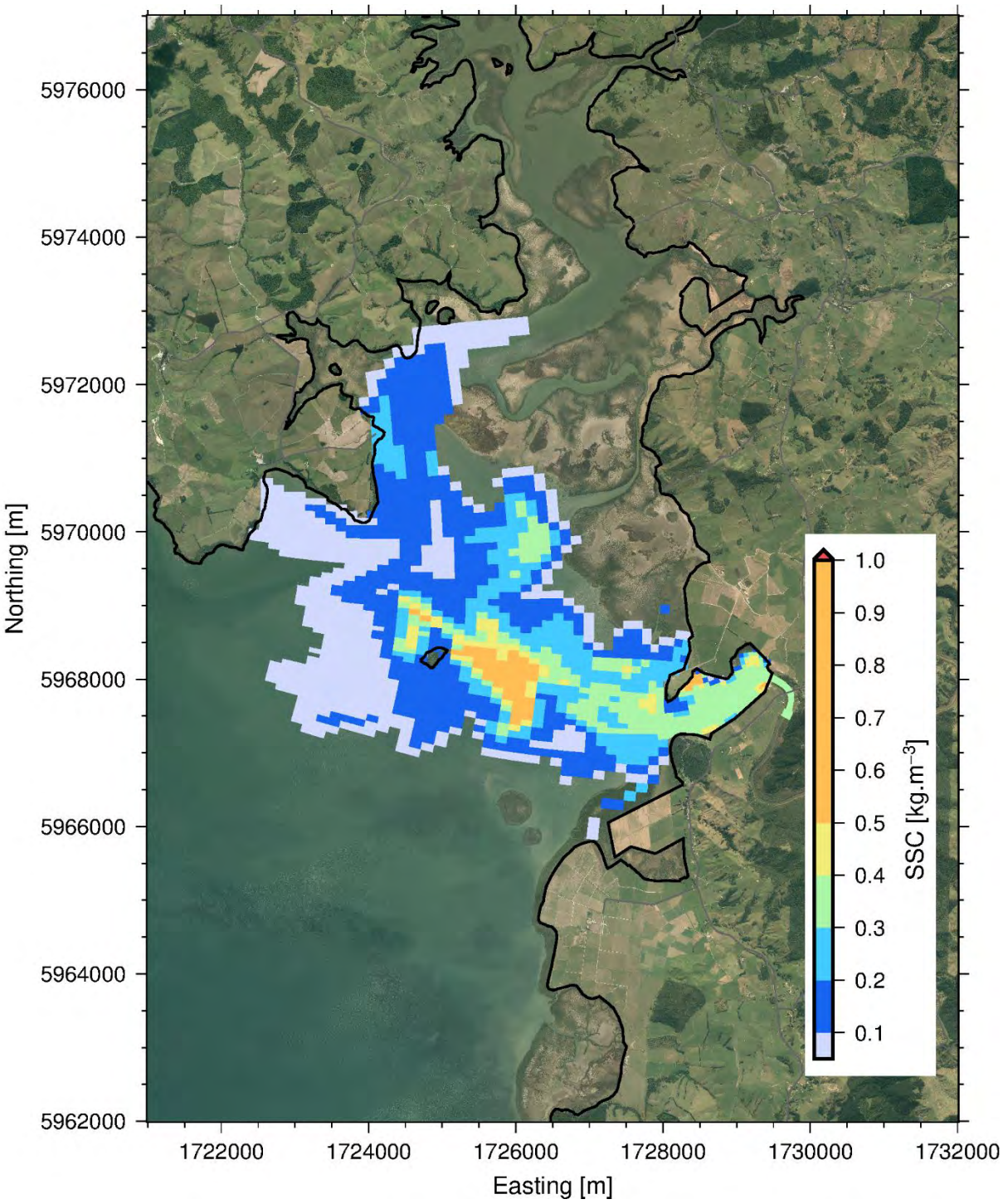

Figure 86: Suspended sediment concentration 1 day after the start of the event for the construction 50-year ARI, SW wind event. Note the start of the event is when the suspended sediment concentration exceeds 0.01 kg/m^3 in the model input.

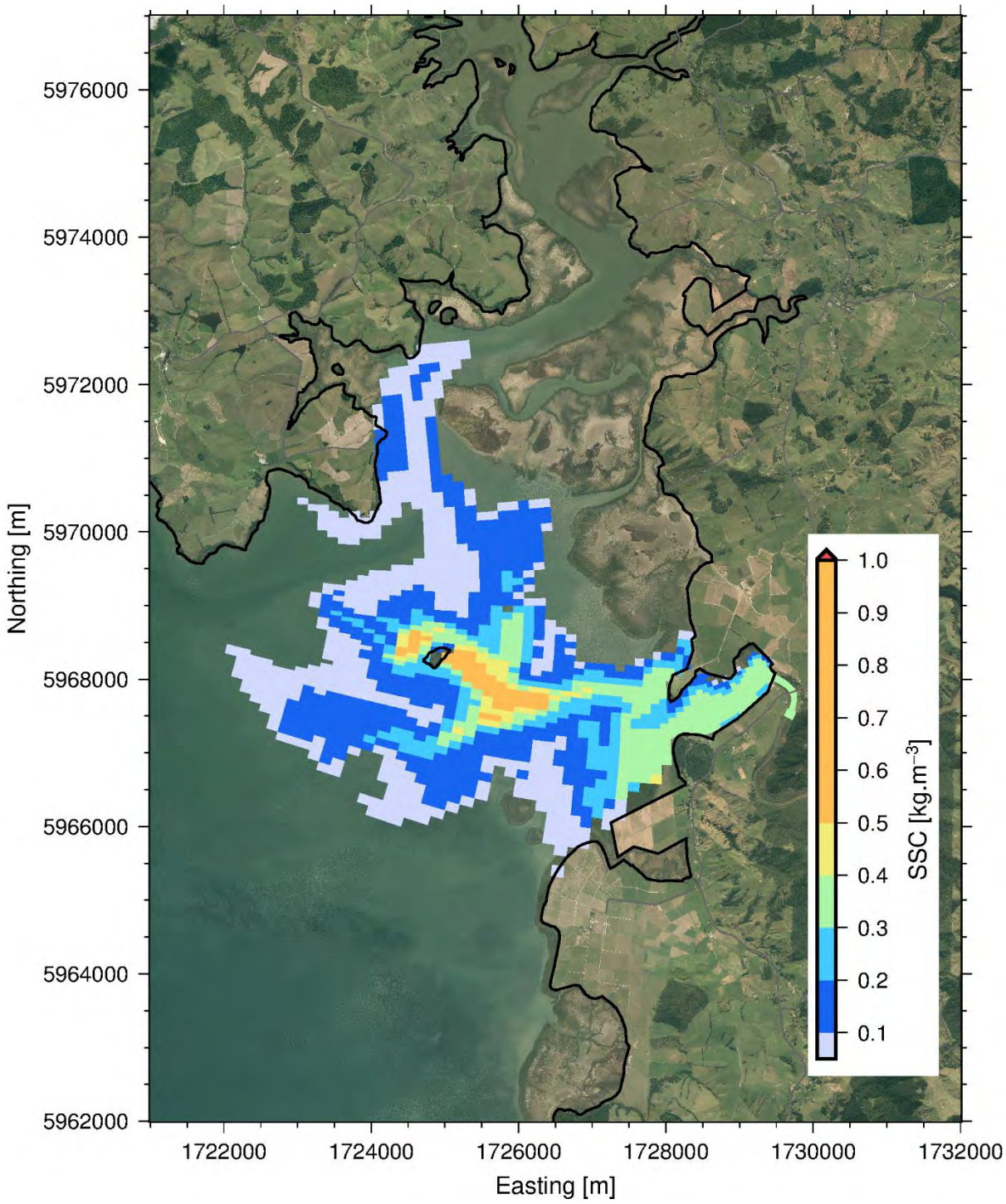

Figure 87: Suspended sediment concentration 1 day after the start of the event for the construction 50-year ARI, NE wind event. Note the start of the event is when the suspended sediment concentration exceeds 0.01 kg/m^3 in the model input.

Suspended sediment concentration 3 days after the start of the event for the construction 50-year ARI event

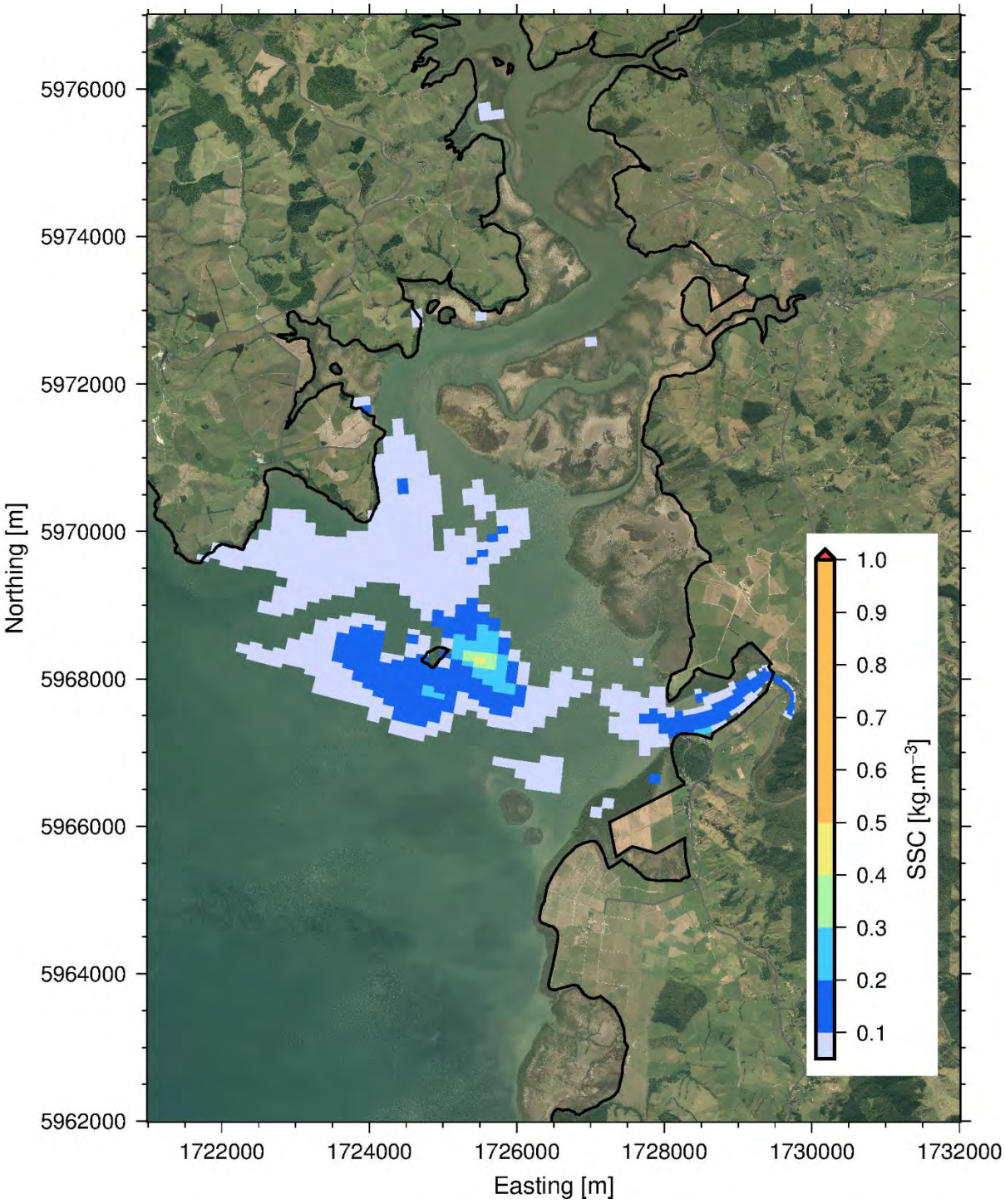

Figure 88: Suspended sediment concentration 3 days after the start of the event for the construction 50-year ARI, calm wind event. Note the start of the event is when the suspended sediment concentration exceeds 0.01 kg/m^3 in the model input.

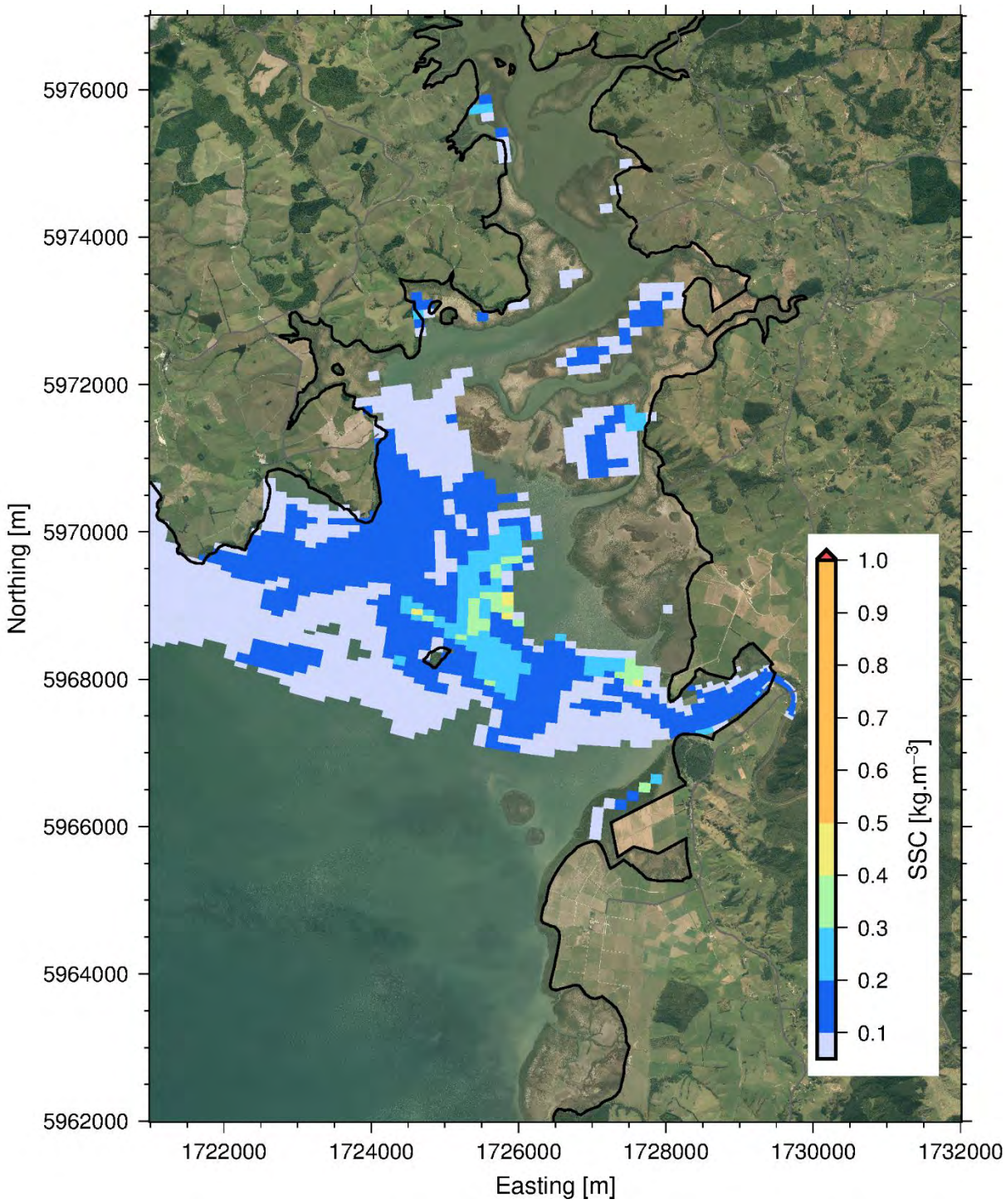

Figure 89: Suspended sediment concentration 3 days after the start of the event for the construction 50-year ARI, SW wind event. Note the start of the event is when the suspended sediment concentration exceeds 0.01 kg/m^3 in the model input.

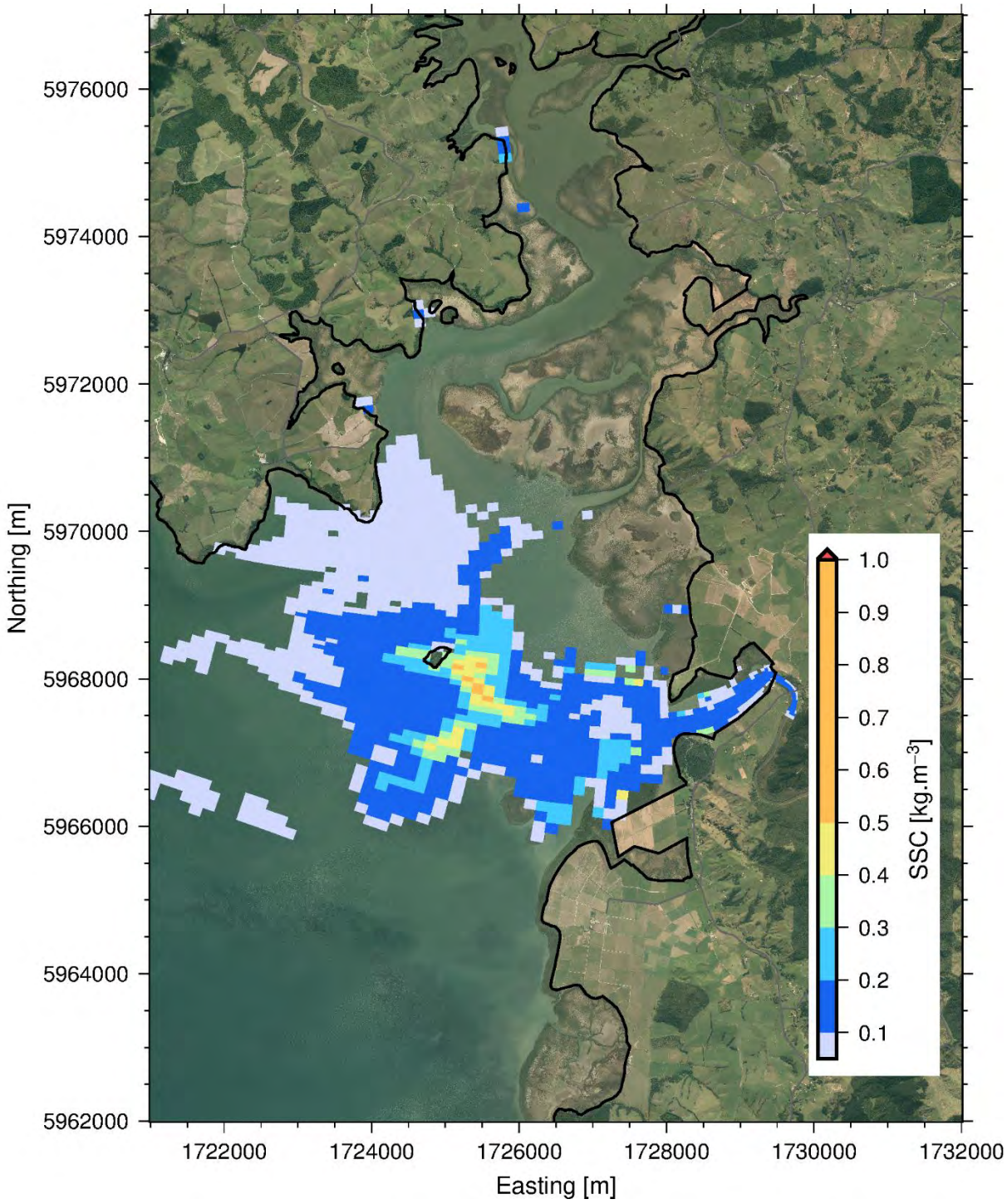

Figure 90: Suspended sediment concentration 3 days after the start of the event for the construction 50-year ARI, NE wind event. Note the start of the event is when the suspended sediment concentration exceeds 0.01 kg/m^3 in the model input.

Maximum continuous time where the SSC exceeds 0.08 kg/m^3 for the construction 10-year ARI event

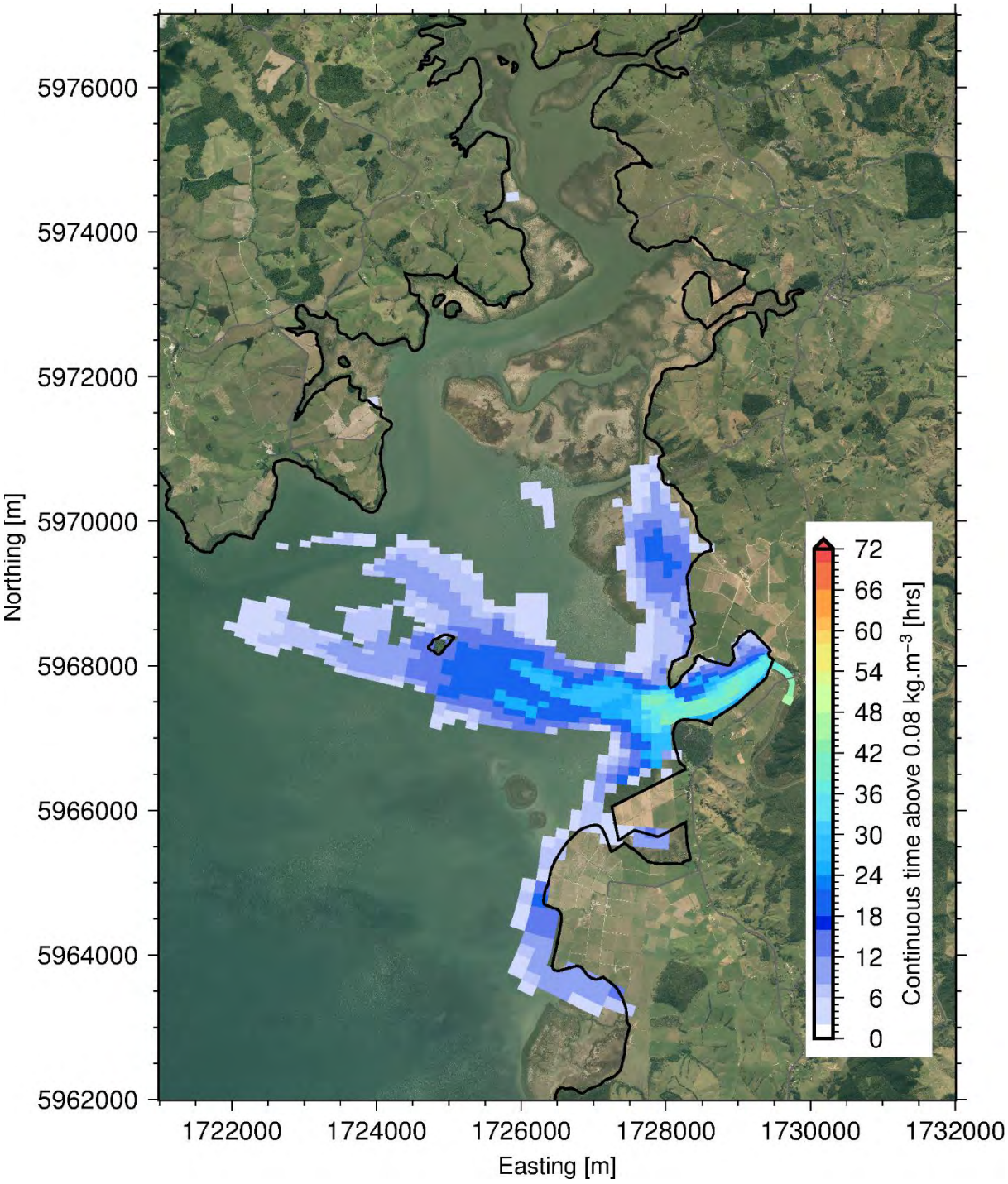

Figure 91: Maximum continuous time where the SSC exceeds 0.08 kg/m^3 for the construction 10-year ARI, calm wind event.

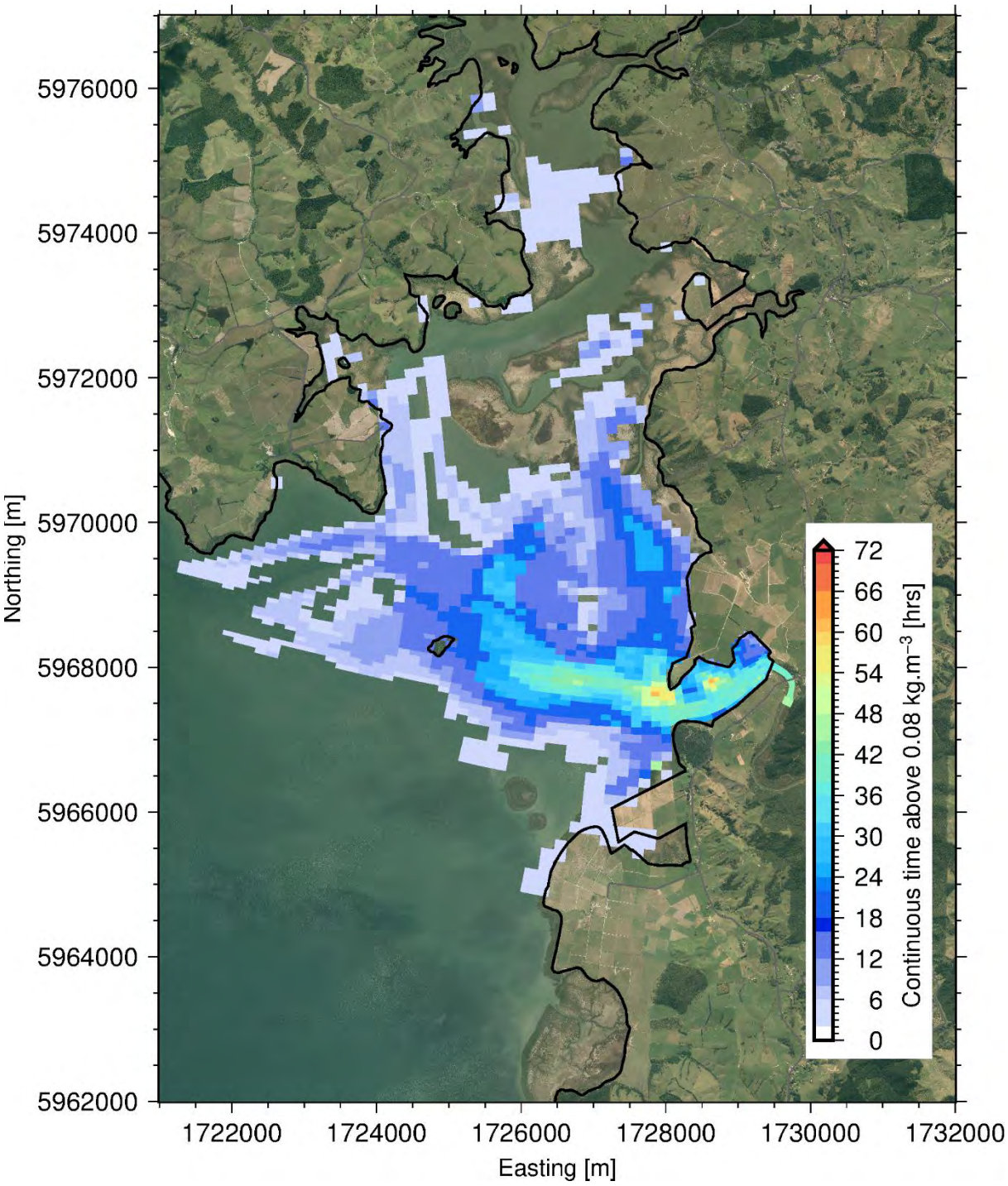

Figure 92: Maximum continuous time where the SSC exceeds 0.08 kg/m^3 for the construction 10-year ARI, SW wind event.

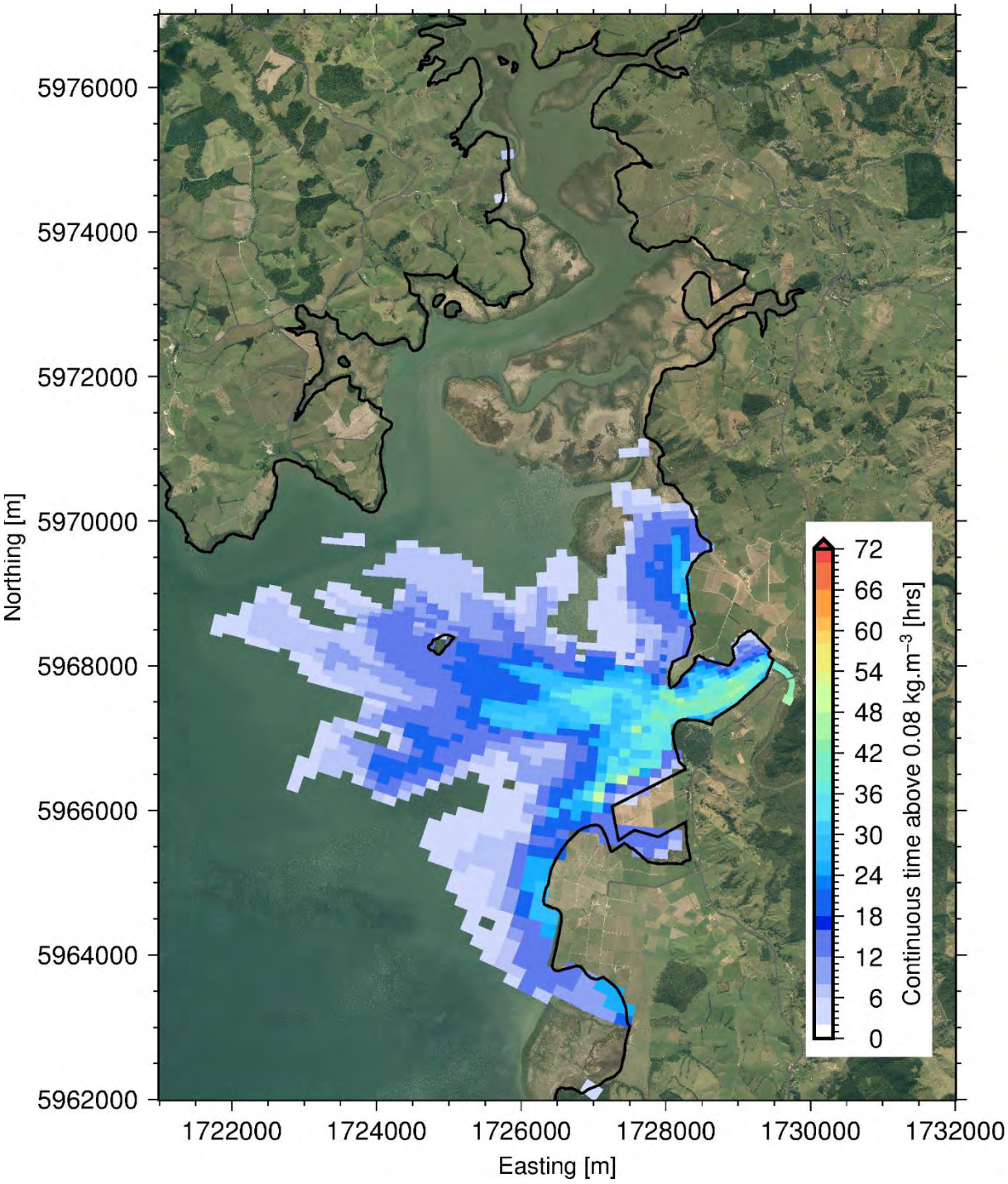

Figure 93: Maximum continuous time where the SSC exceeds 0.08 kg/m^3 for the construction 10-year ARI, NE wind event.

Maximum continuous time where the SSC exceeds 0.08 kg/m^3 for the construction 50-year ARI event

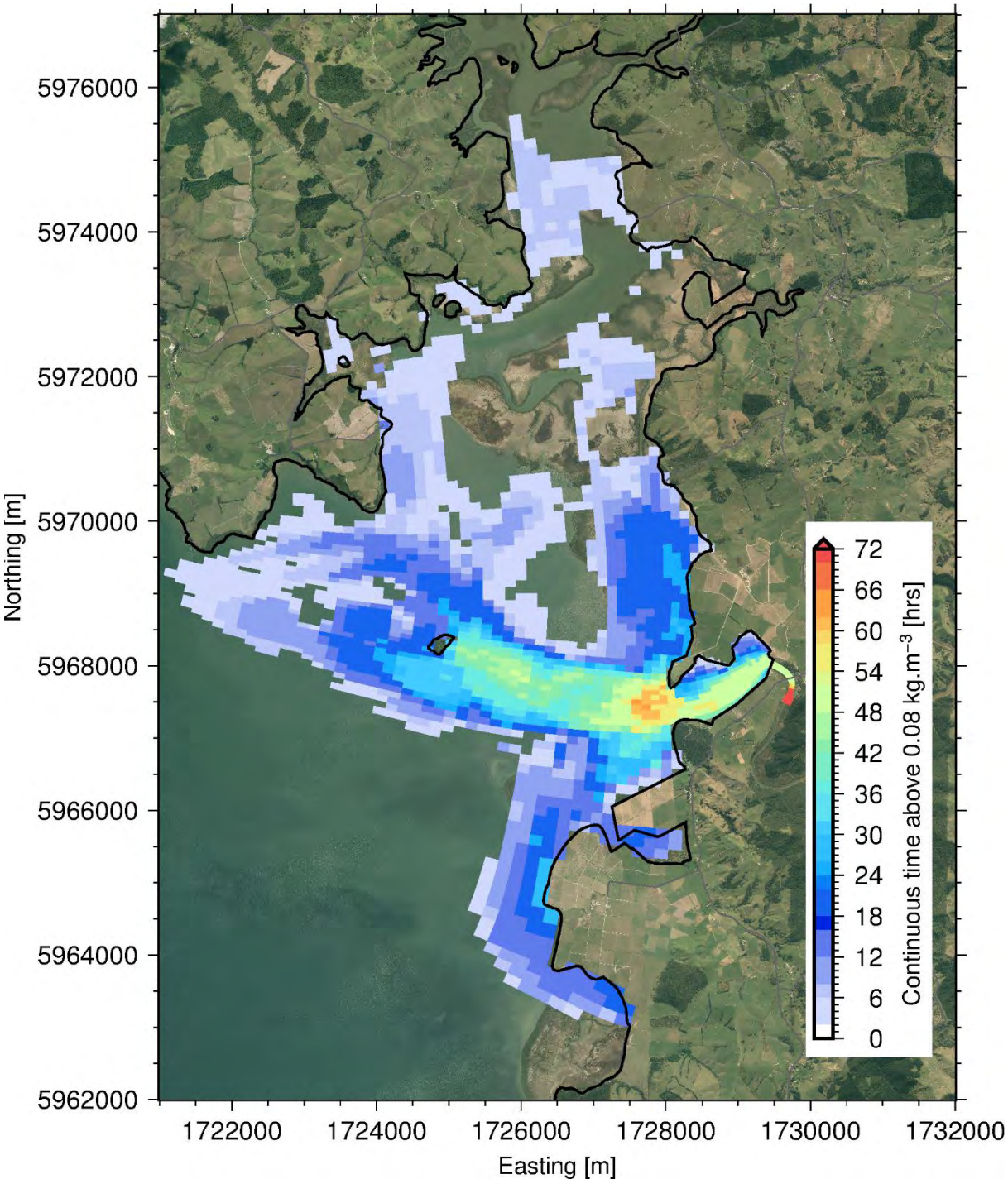

Figure 94: Maximum continuous time where the SSC exceeds 0.08 kg/m^3 for the construction 50-year ARI, calm wind event.

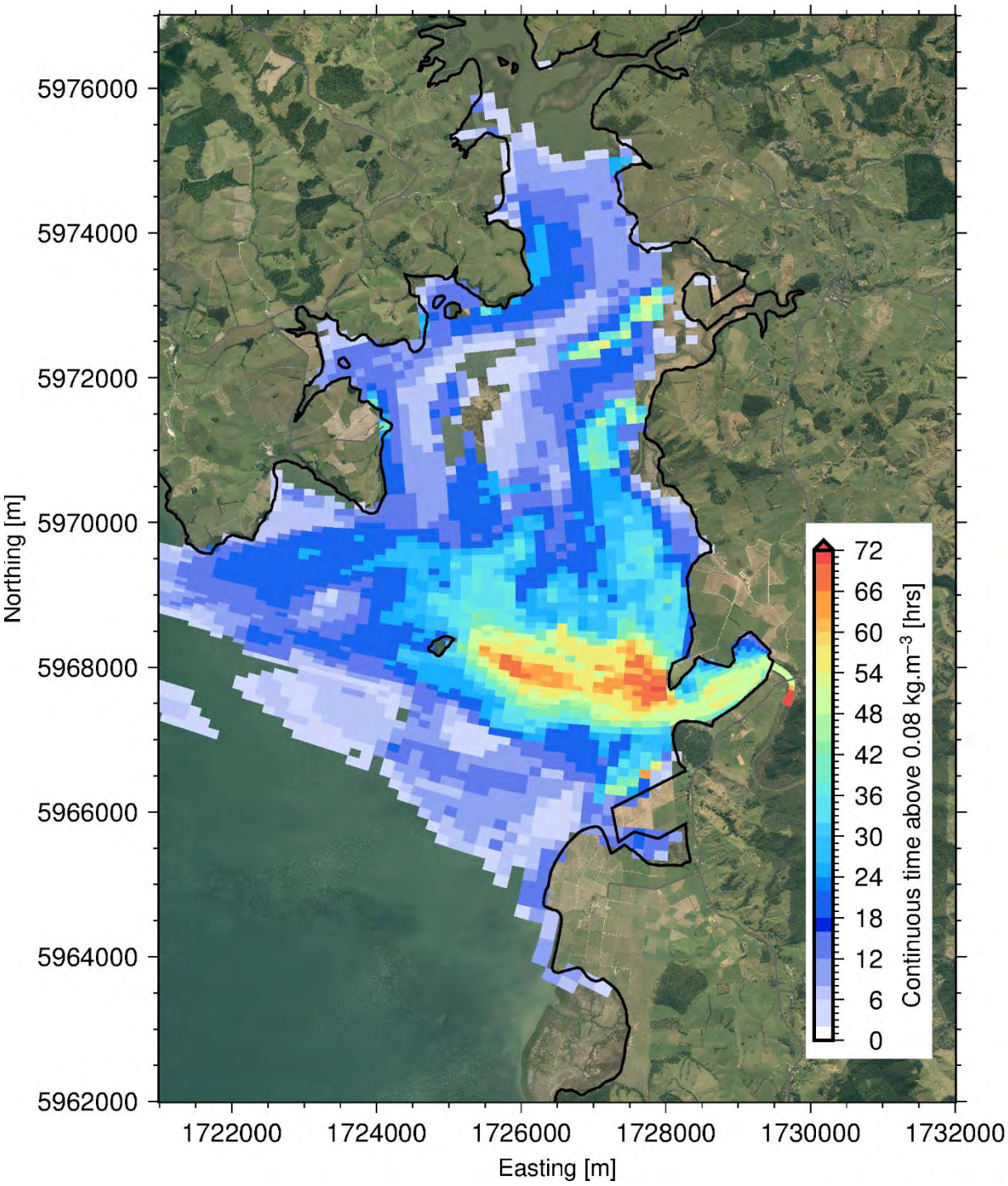

Figure 95: Maximum continuous time where the SSC exceeds 0.08 kg/m^3 for the construction 50-year ARI, SW wind event.

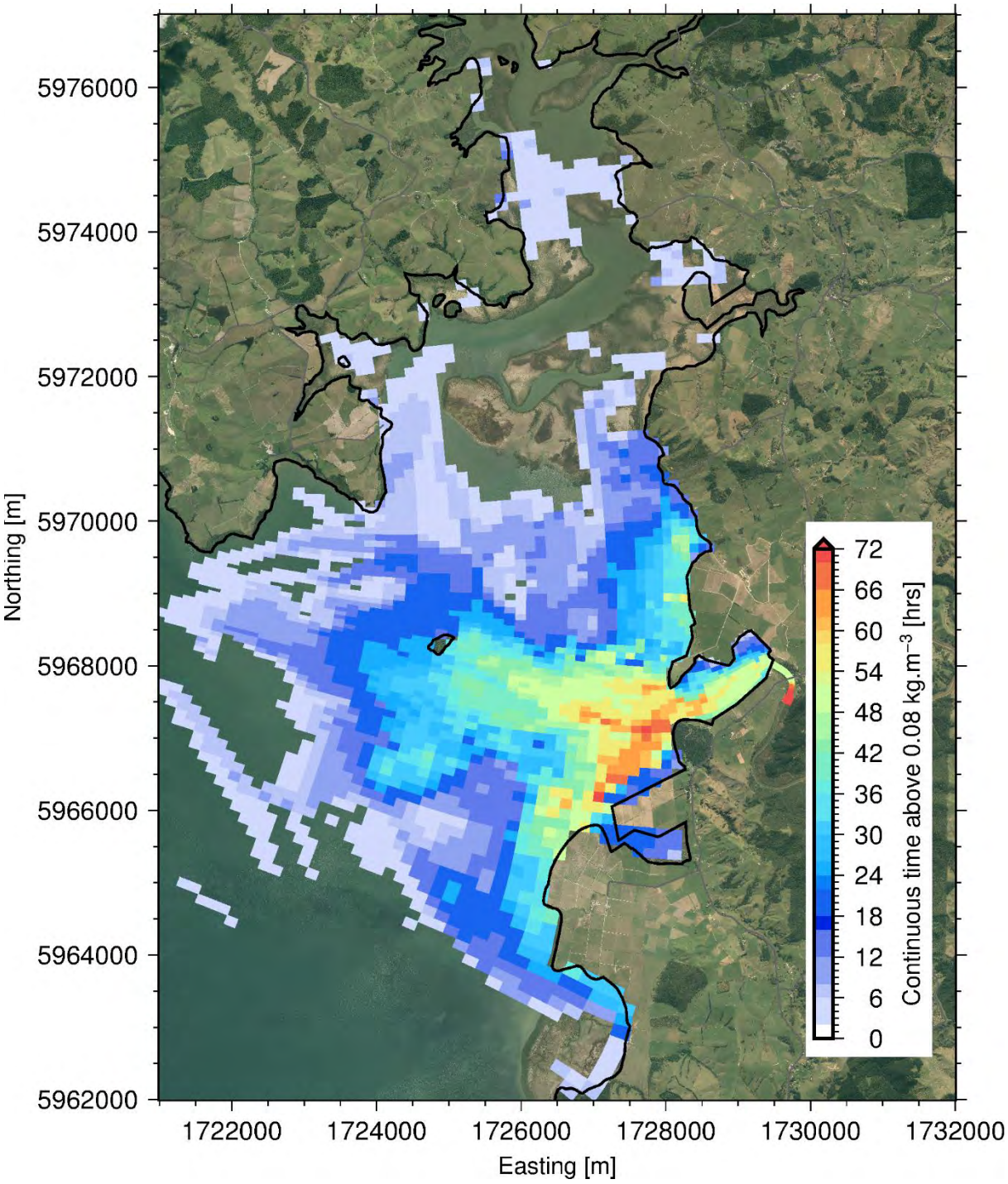

Figure 96: Maximum continuous time where the SSC exceeds 0.08 kg/m^3 for the construction 50-year ARI, NE wind event.

Sediment deposition depth 3 days after the start of the event for the construction 10-year ARI event

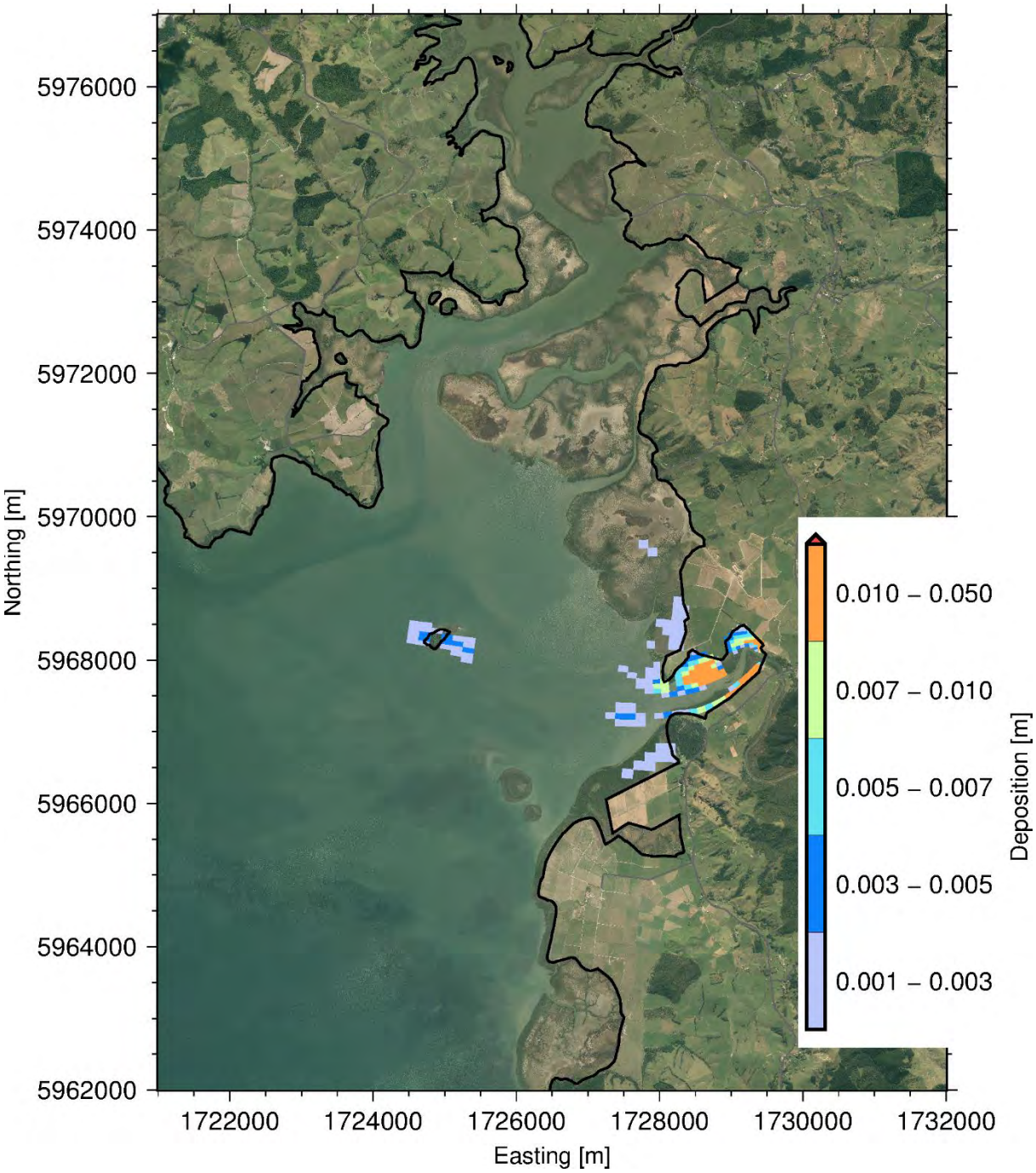

Figure 97: Sediment deposition depth 3 days after the start of the event for the construction 10-year ARI, calm wind event.

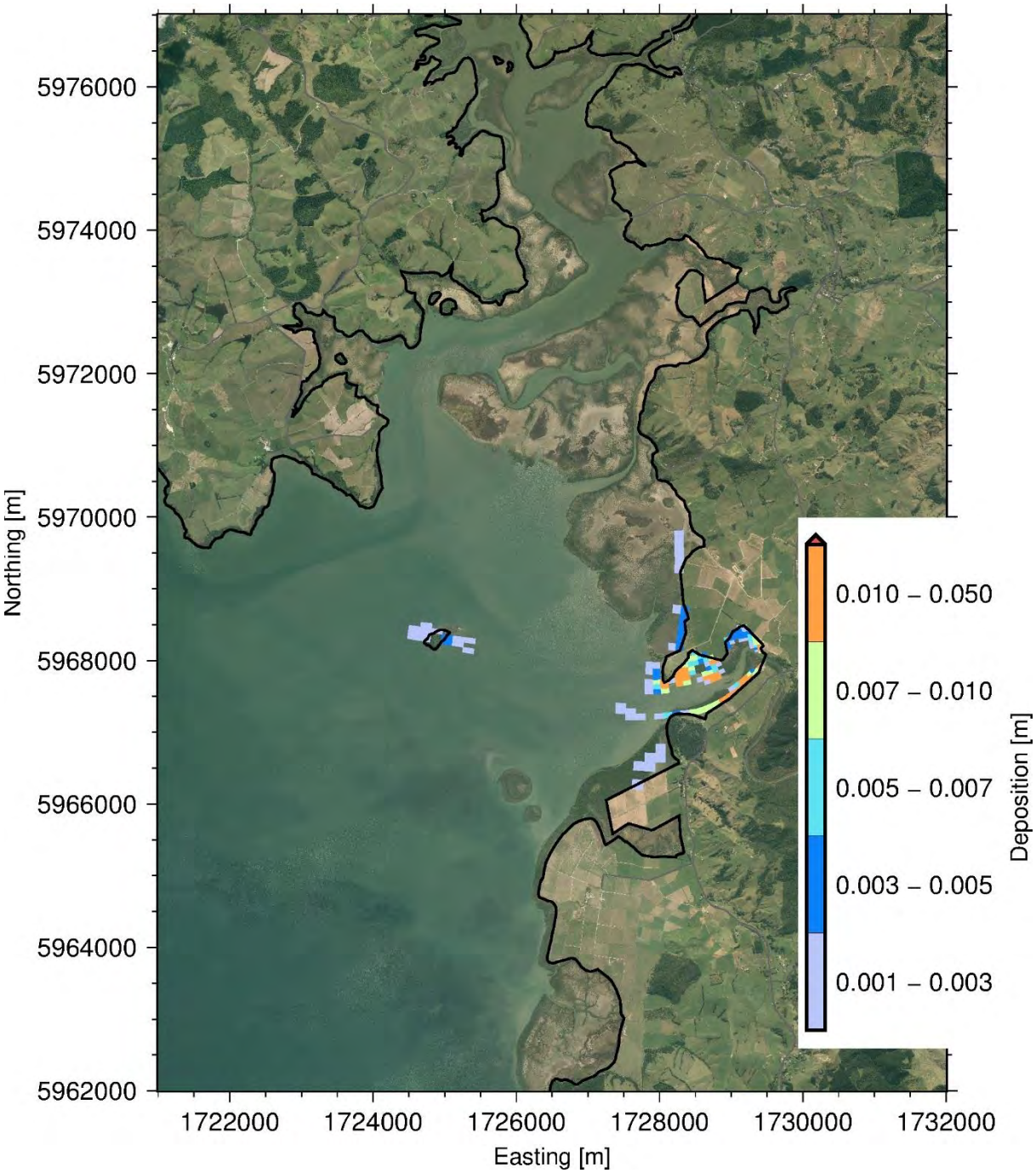

Figure 98: Sediment deposition depth 3 days after the start of the event for the construction 10-year ARI, SW wind event. Note: deposition lower than 0.001 m are not shown here.

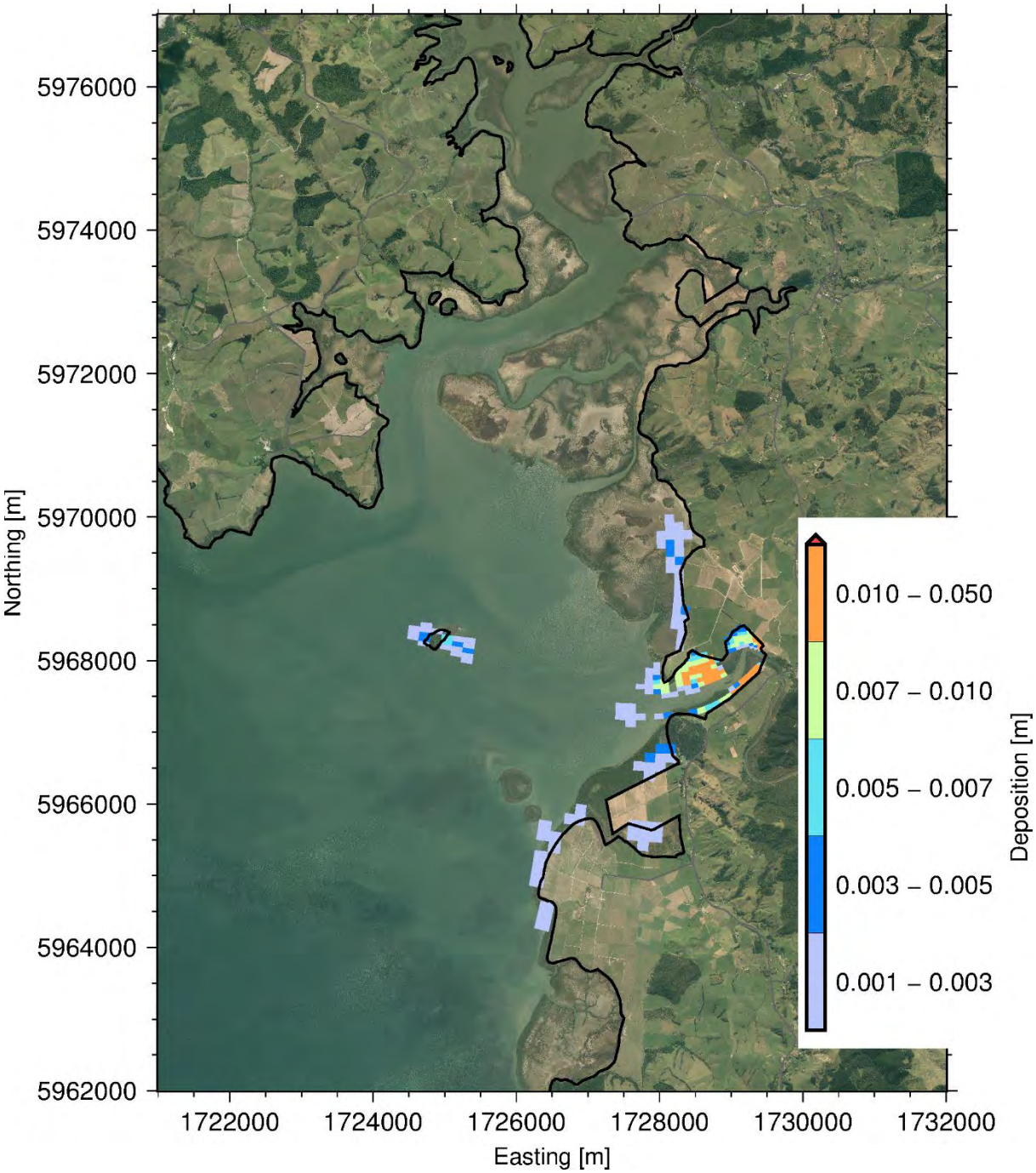

Figure 99: Sediment deposition depth 3 days after the start of the event for the construction 10-year ARI, NE wind event. Note: deposition lower than 0.001 m are not shown here.

Sediment deposition depth 3 days after the start of the event for the construction 50-year ARI event

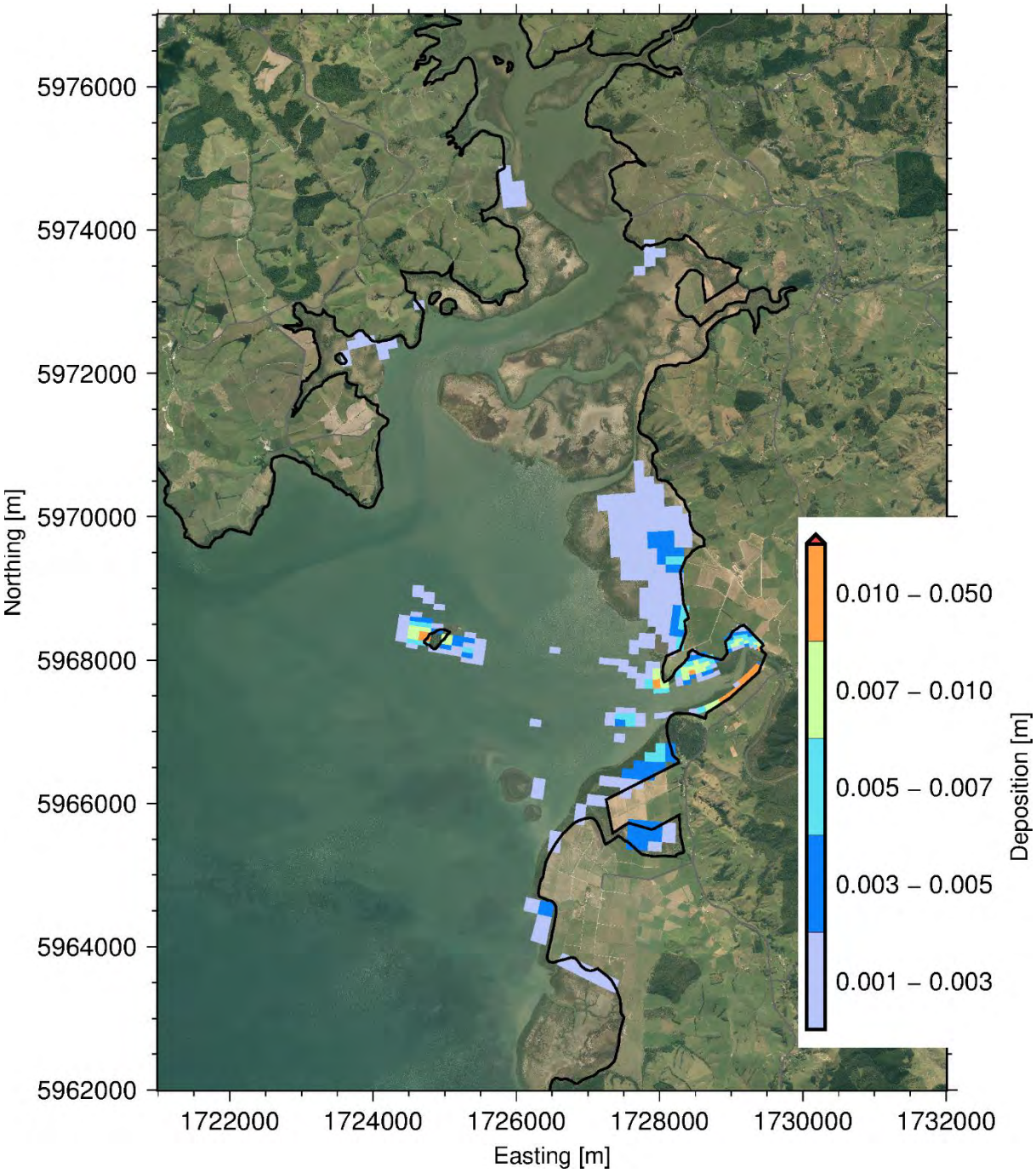

Figure 100: Sediment deposition depth 3 days after the start of the event for the construction 50-year ARI, calm wind event. Note: deposition lower than 0.001 m are not shown here.

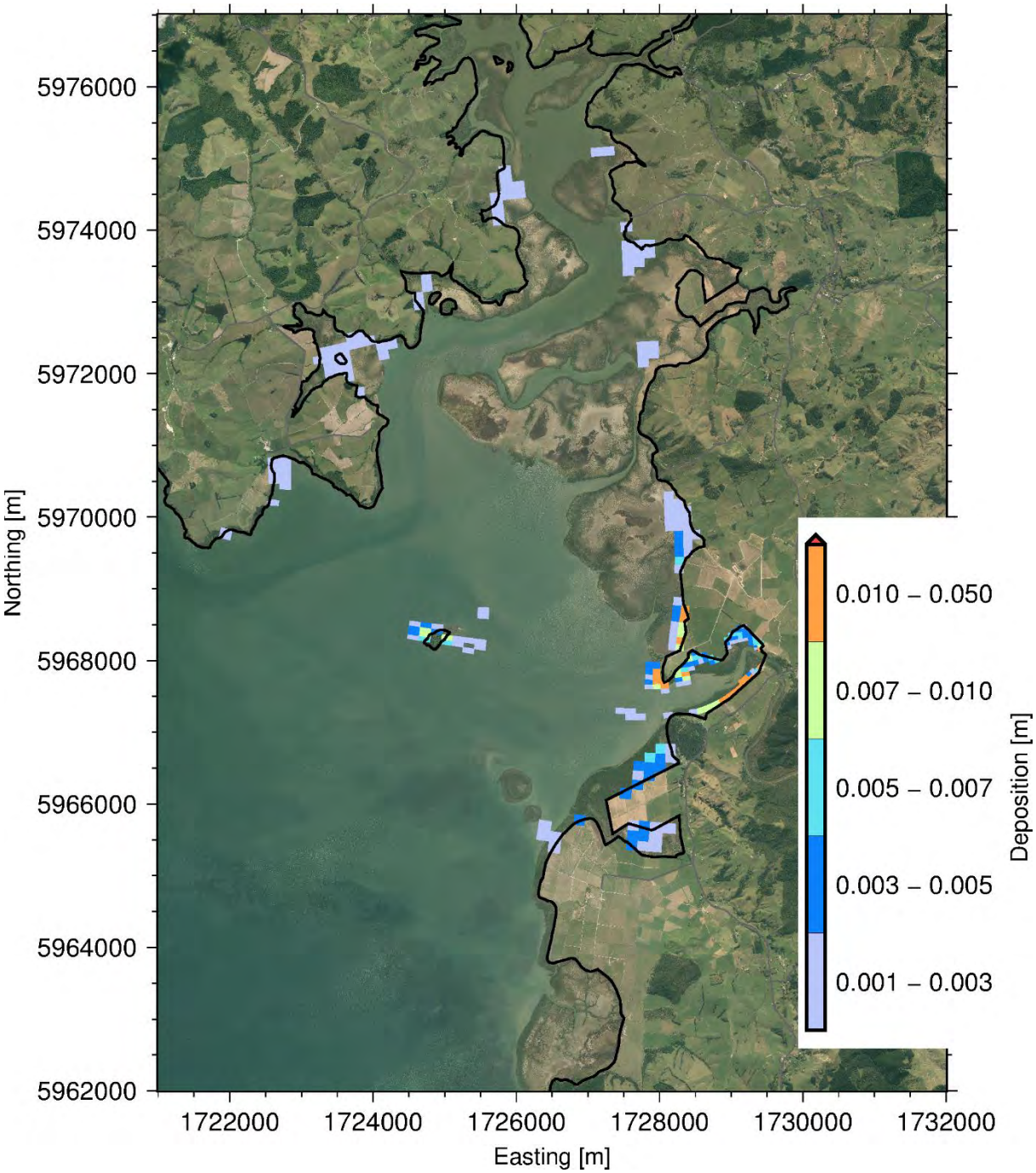

Figure 101: Sediment deposition depth 3 days after the start of the event for the construction 50-year ARI, SW wind event. Note: deposition lower than 0.001 m are not shown here.

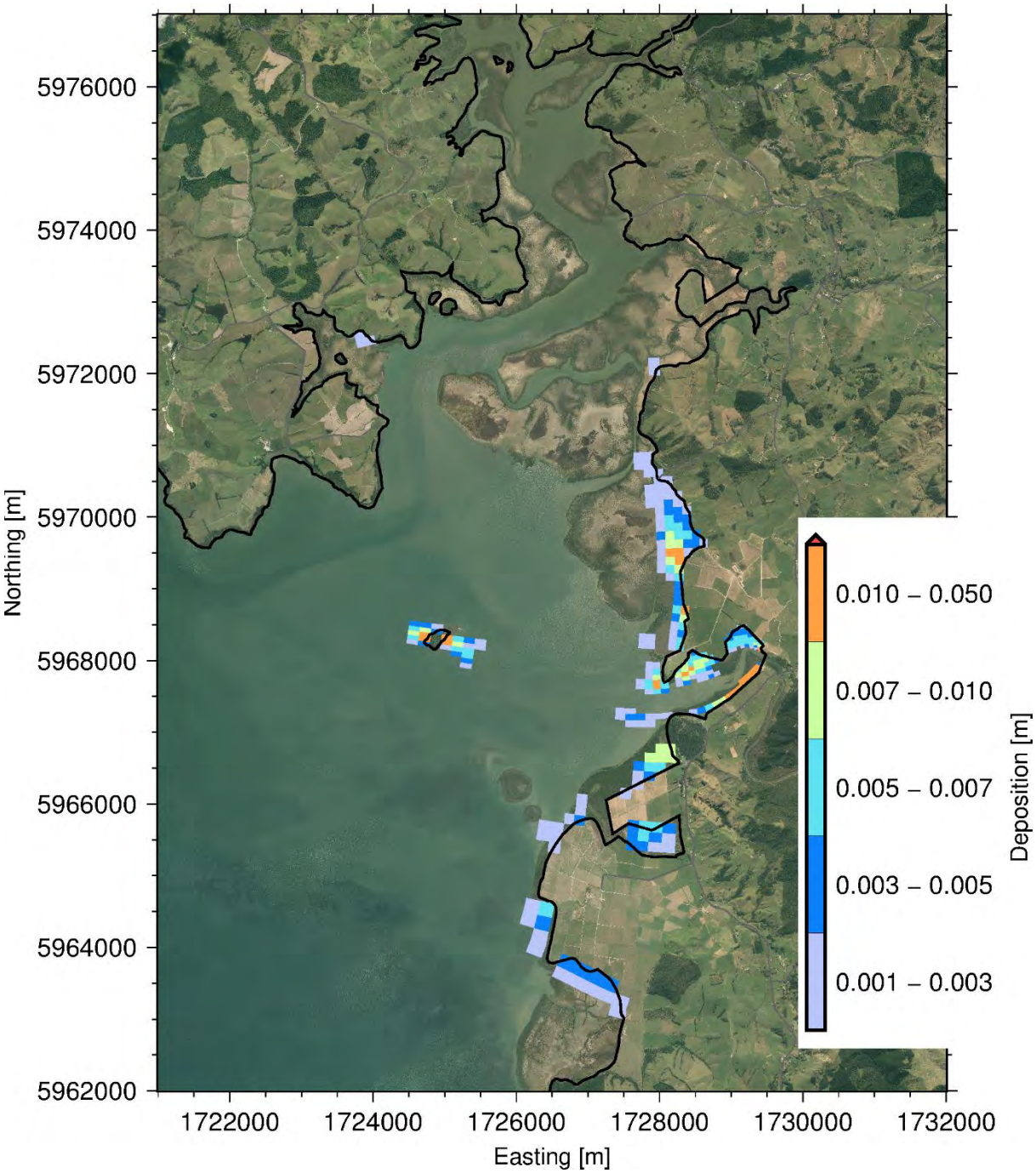

Figure 102: Sediment deposition depth 3 days after the start of the event for the construction 50-year ARI, NE wind event. Note: deposition lower than 0.001 m are not shown here.

Sediment deposition depth at the end of simulation for the construction 10-year ARI event

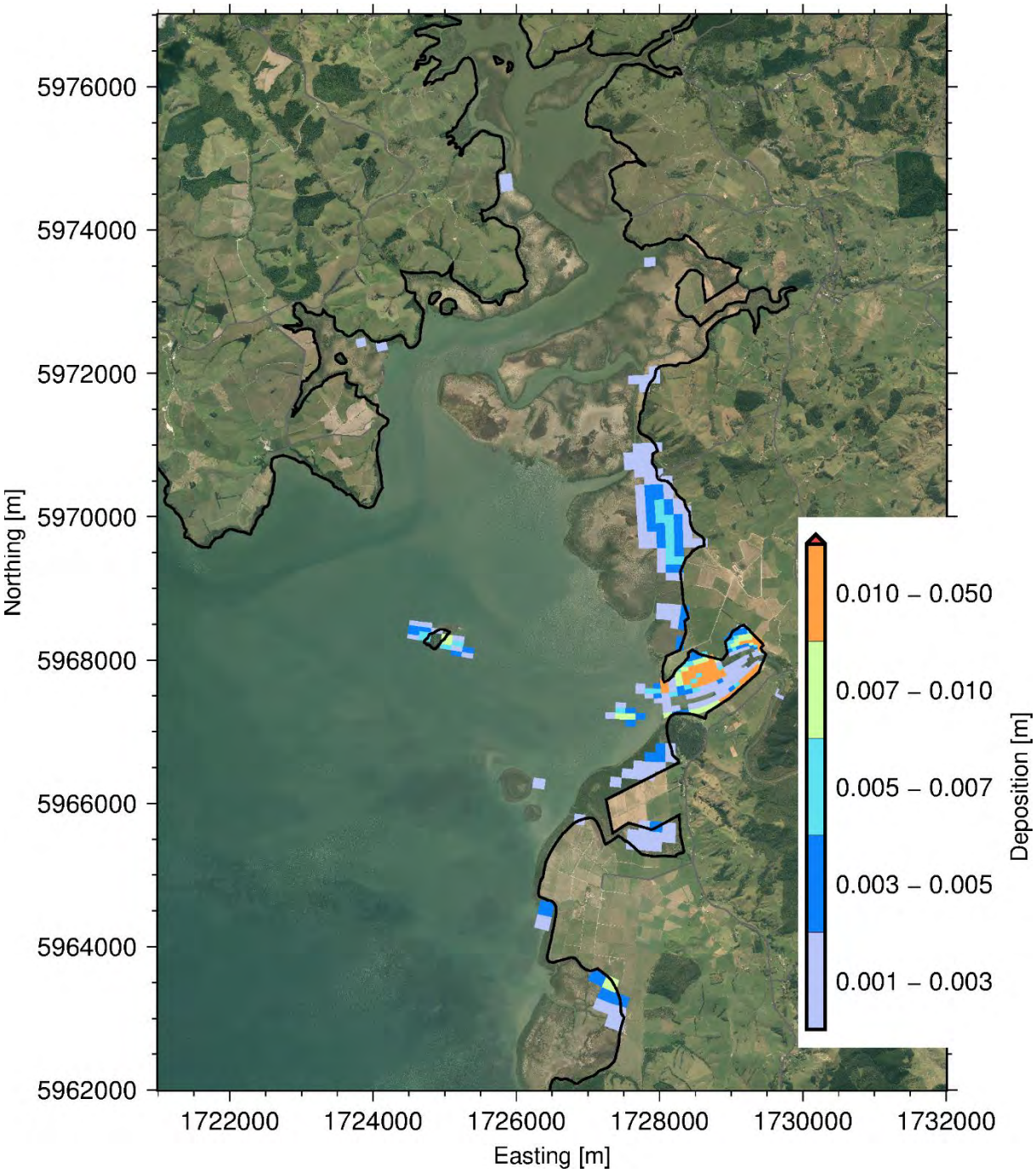

Figure 103: Sediment deposition depth at the end of simulation for the construction 10-year ARI, calm wind event. Note: deposition lower than 0.001 m are not shown here.

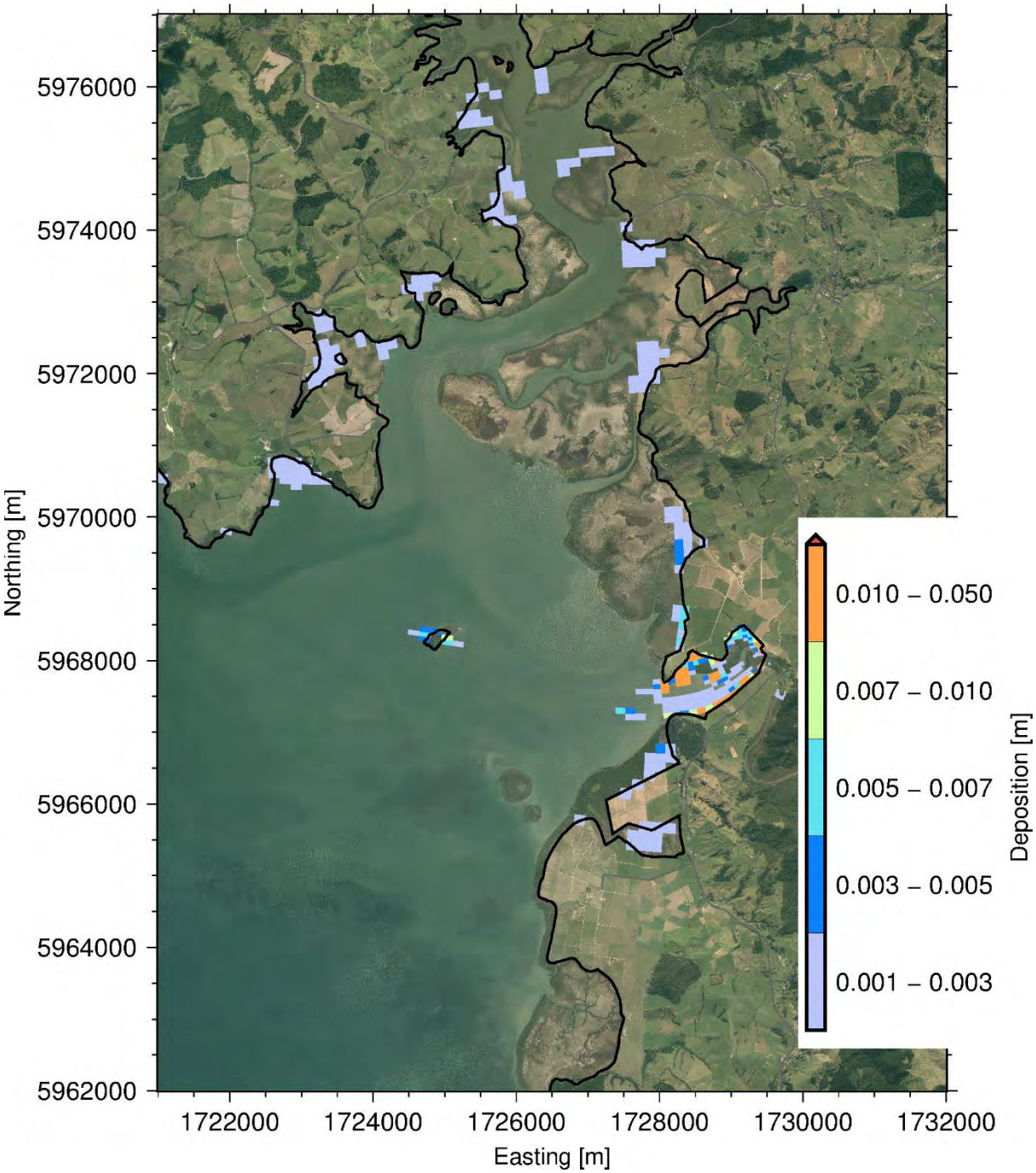

Figure 104: Sediment deposition depth at the end of simulation for the construction 10-year ARI, SW wind event Note: deposition lower than 0.001 m are not shown here..

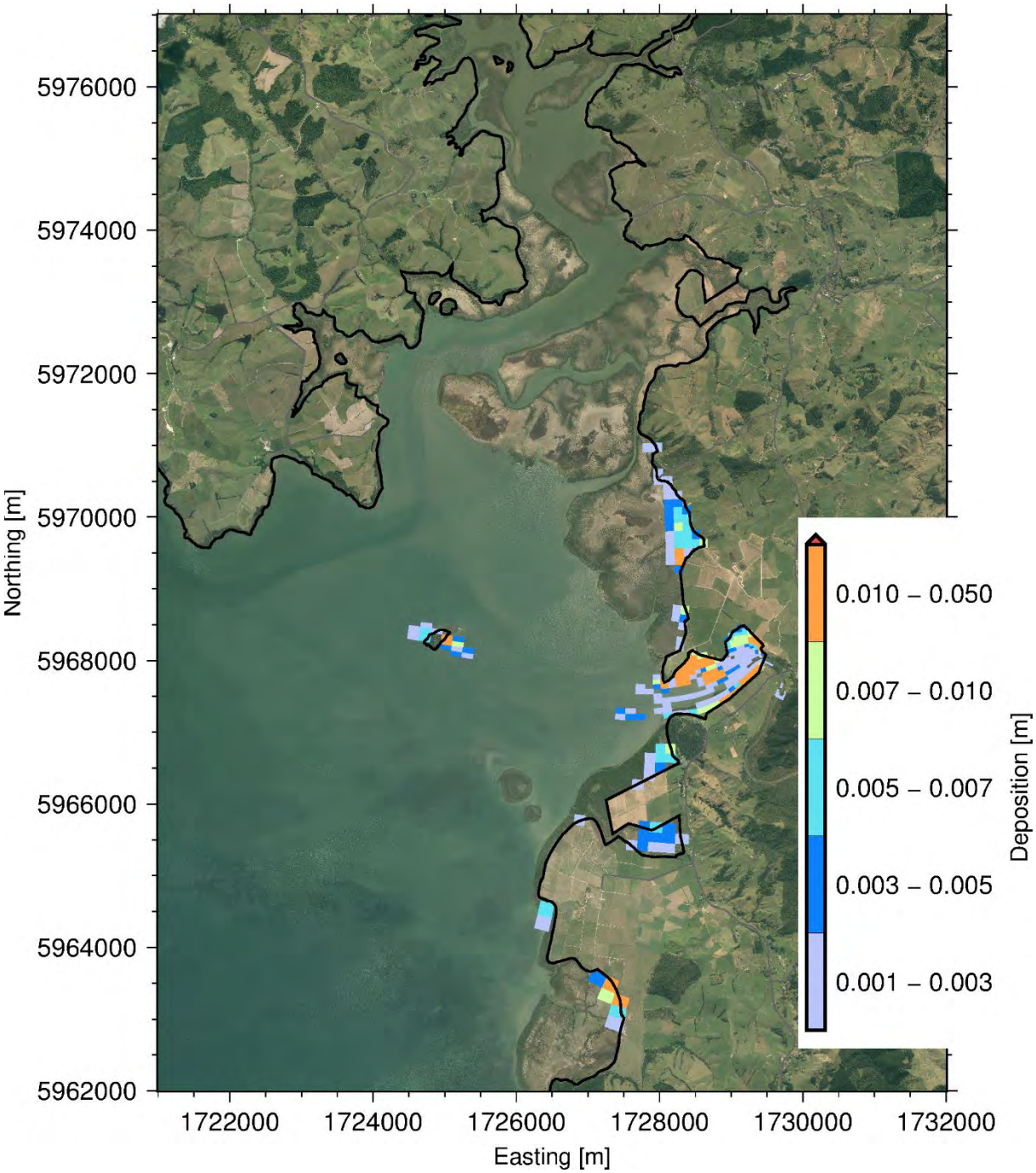

Figure 105: Sediment deposition depth at the end of simulation for the construction 10-year ARI, NE wind event. Note: deposition lower than 0.001 m are not shown here.

Sediment deposition depth at the end of simulation for the construction 50-year ARI event

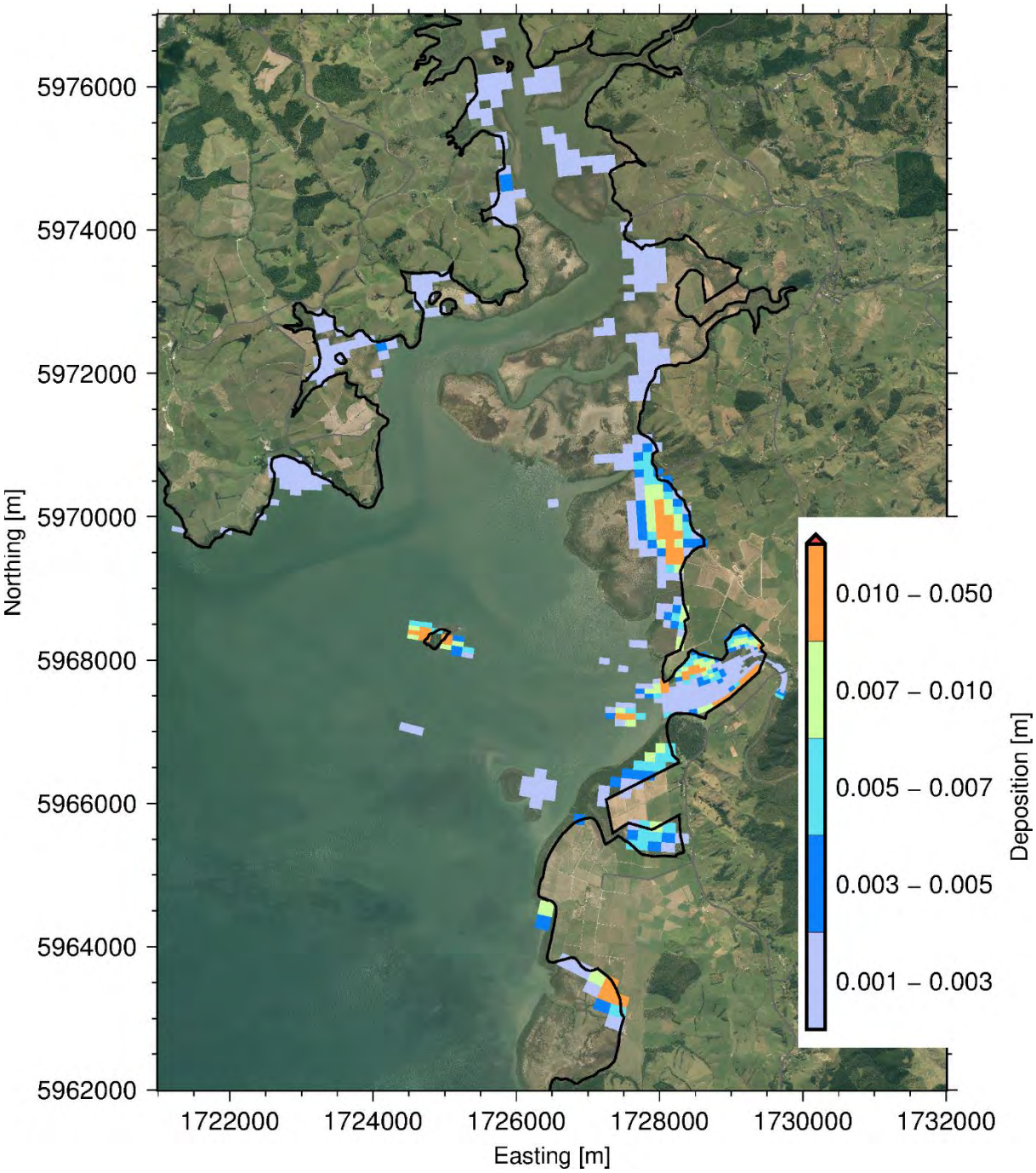

Figure 106: Sediment deposition depth at the end of simulation for the construction 50-year ARI, calm wind event. Note: deposition lower than 0.001 m are not shown here.

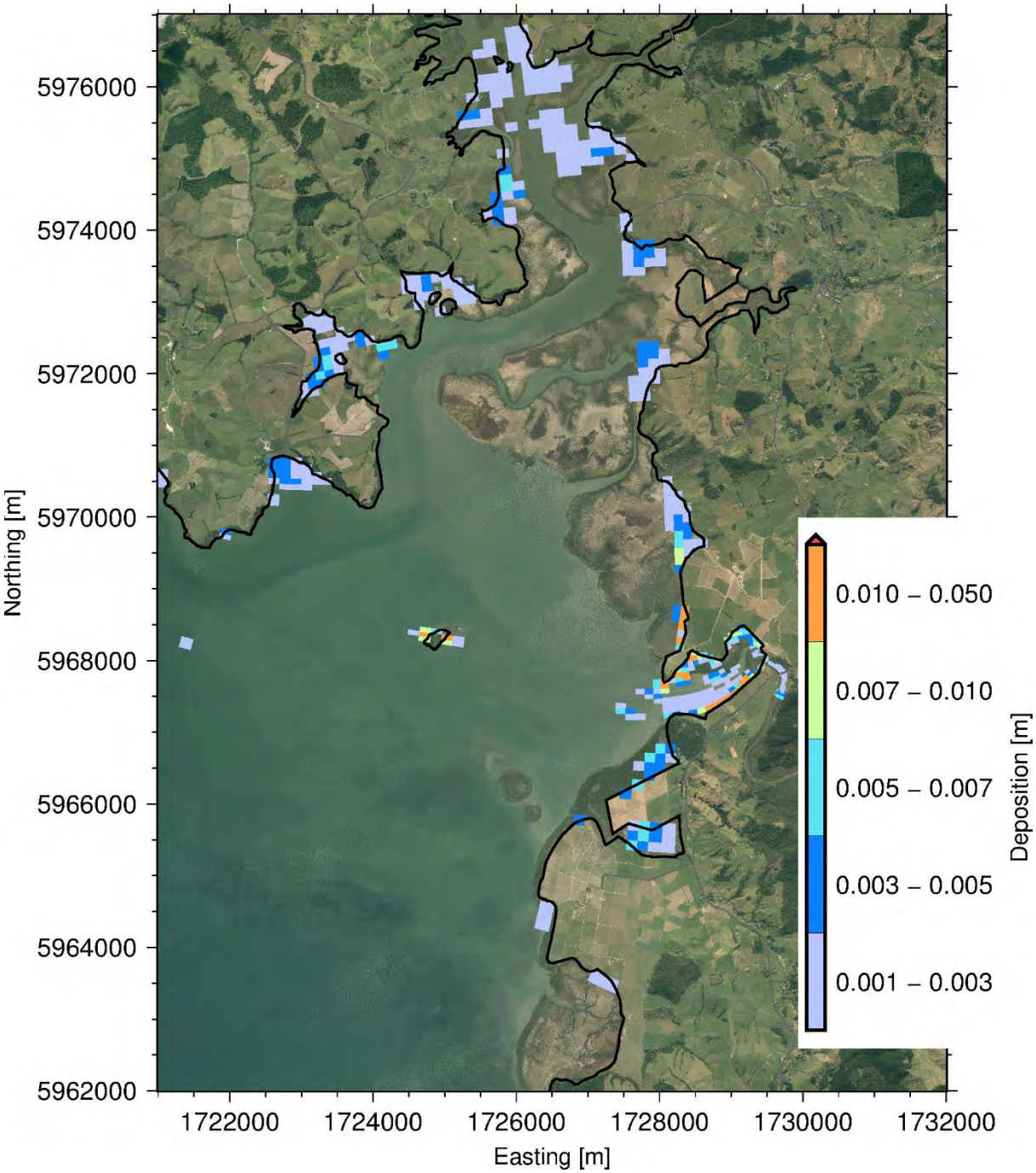

Figure 107: Sediment deposition depth at the end of simulation for the construction 50-year ARI, SW wind event. Note: deposition lower than 0.001 m are not shown here.

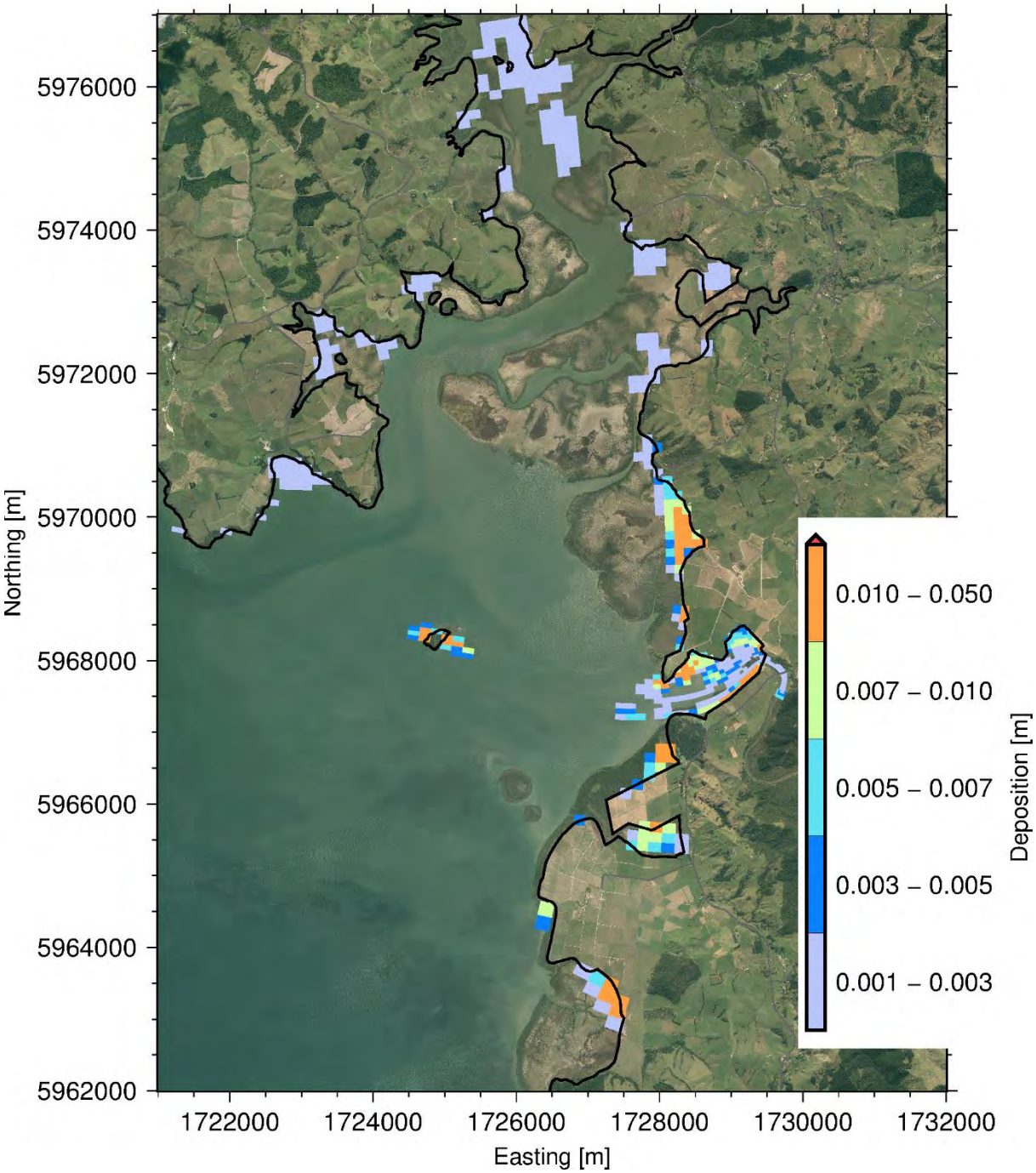

Figure 108: Sediment deposition depth at the end of simulation for the construction 50-year ARI, NE wind event. Note: deposition lower than 0.001 m are not shown here.

APPENDIX D: DIFFERENCE BETWEEN BASELINE AND CONSTRUTION SIMULATIONS

Tables of change to area receiving deposition at the end of the 7-day simulation for the 10-year ARI events

Table 14: Deposition areas for 10-year ARI, calm wind event

Deposition depth range	Area covered by sediment in each deposition range (ha)			
	Baseline	Construction	Difference	Difference (%)
0.02 – 1 mm	2251	2269	17.9	0.8%
1 – 3 mm	181	187	5.3	2.9%
3 - 5 mm	79	77	-2.1	-2.7%
5 – 7 mm	25	29	4.2	16.7%
7 – 10 mm	18	20	1.2	6.4%
> 10 mm	23	25	2.3	10.0%
Total > 0.02 mm	2578	2607	28.8	1.1%
Total > 1 mm	327	337	10.9	3.3%
Total > 3 mm	145	151	5.5	3.8%

Table 15: Deposition areas for 10-year ARI, SW wind event

Deposition depth range	Area covered by sediment in each deposition depth range (ha)			
	Baseline	Construction	Difference	Difference (%)
0.02 – 1 mm	1560	1566	6.1	0.4%
1 – 3 mm	252	273	20.6	8.2%
3 - 5 mm	15	19	3.4	22.6%
5 – 7 mm	13	14	1.3	10.0%

7 – 10 mm	7	7	-0.4	-5.4%
> 10 mm	18	19	0.9	4.9%
Total > 0.02 mm	1865	1897	31.9	1.7%
Total > 1 mm	305	331	25.8	8.5%
Total > 3 mm	53	58	5.2	9.8%

Table 16: Deposition areas for 10-year ARI, NE wind event

Deposition depth range	Area covered by sediment in each deposition range (ha)			
	Baseline	Construction	Difference	Difference (%)
0.02 – 1 mm	1658	1705	47.2	2.8%
1 – 3 mm	101	101	0.4	0.4%
3 - 5 mm	51	47	-4.0	-7.8%
5 – 7 mm	32	36	3.9	12.1%
7 – 10 mm	18	20	2.7	15.5%
> 10 mm	36	38	1.7	4.7%
Total > 0.02 mm	1897	1949	52.0	2.7%
Total > 1 mm	239	243	4.8	2.0%
Total > 3 mm	138	142	4.4	3.2%

Tables of change to area receiving deposition at the end of the 7-day simulation for the 50-year ARI events

Table 17: Deposition areas for 50-year ARI, calm wind event

Deposition depth range	Area covered by sediment in each deposition range (ha)			
	Baseline	Construction	Difference	Difference (%)
0.02 – 1 mm	2823	2906	83.0	2.9%
1 – 3 mm	410	451	40.3	9.8%
3 - 5 mm	84	78	-5.9	-7.1%
5 – 7 mm	65	67	1.9	2.9%
7 – 10 mm	58	59	1.0	1.8%
> 10 mm	30	51	21.0	69.2%
Total > 0.02 mm	3470	3611	141.3	4.1%
Total > 1 mm	647	706	58.3	9.0%
Total > 3 mm	237	255	18.0	7.6%

Table 18: Deposition areas for 50-year ARI, SW wind event

Deposition depth range	Area covered by sediment in each deposition range (ha)			
	Baseline	Construction	Difference	Difference (%)
0.02 – 1 mm	1803	1848	45.4	2.5%
1 – 3 mm	380	401	21.2	5.6%
3 - 5 mm	112	111	-0.8	-0.7%
5 – 7 mm	20	40	19.4	95.6%
7 – 10 mm	11	12	0.8	7.6%
> 10 mm	13	17	4.3	33.3%
Total > 0.02 mm	2339	2429	90.4	3.9%

Total > 1 mm	536	581	45.0	8.4%
Total > 3 mm	156	180	23.8	15.2%

Table 19: Deposition areas for 50-year ARI, NE wind event

Deposition depth range	Area covered by sediment in each deposition range (ha)			
	Baseline	Construction	Difference	Difference (%)
0.02 – 1 mm	2102	2128	26.0	1.2%
1 – 3 mm	352	414	62.7	17.8%
3 - 5 mm	44	42	-2.0	-4.5%
5 – 7 mm	39	40	1.5	3.9%
7 – 10 mm	44	44	-0.1	-0.2%
> 10 mm	52	63	11.7	22.8%
Total > 0.02 mm	2633	2733	99.9	3.8%
Total > 1 mm	530	604	73.9	13.9%
Total > 3 mm	179	190	11.2	6.2%

Additional deposition arising from Project construction at 3-days after the start of the event for the 10-year ARI events

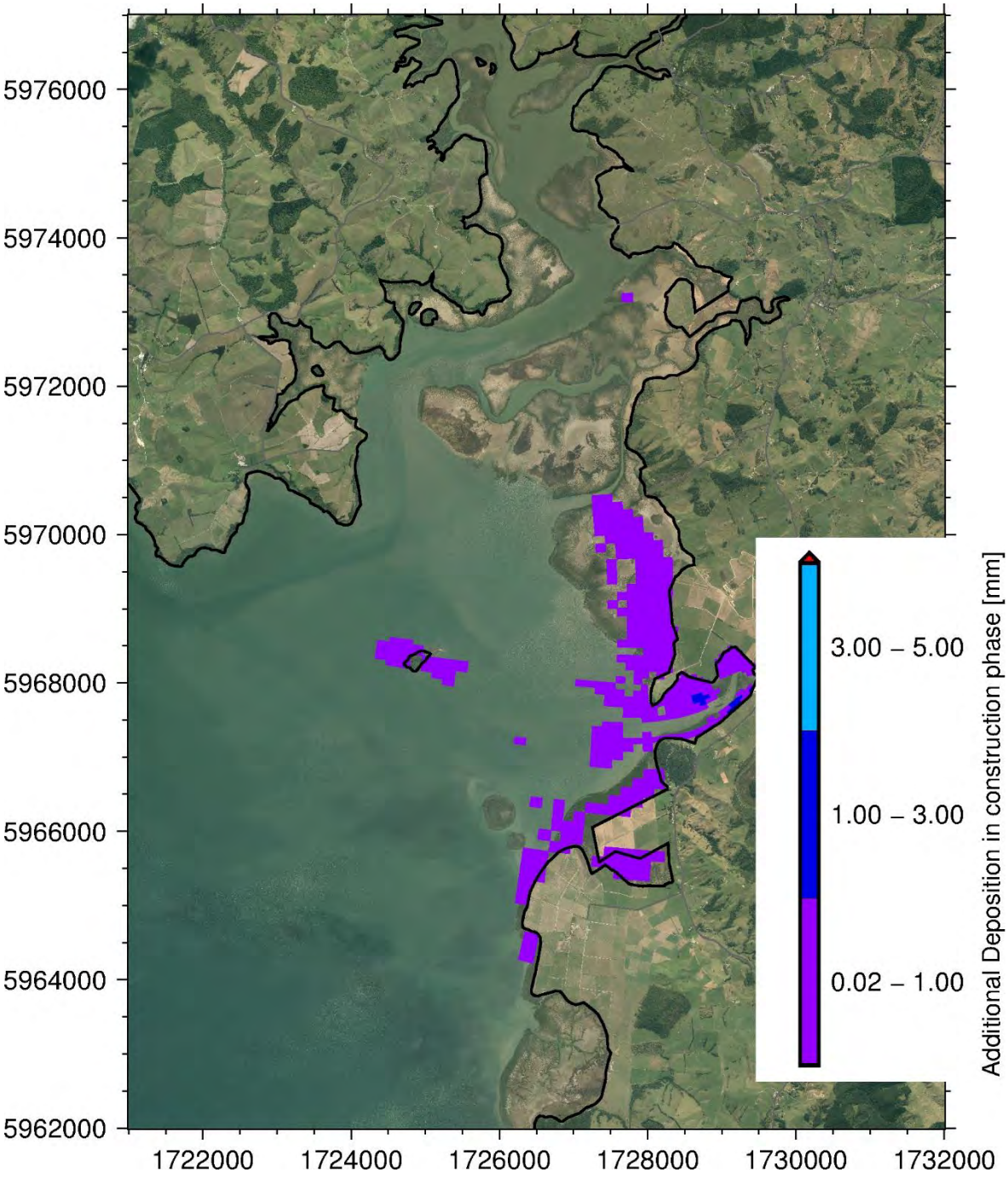

Figure 109: Additional deposition arising from Project construction at 3 days after the start of the event for the 10-year ARI, calm wind event. Note: additional deposition lower than 0.02 mm are not shown here.

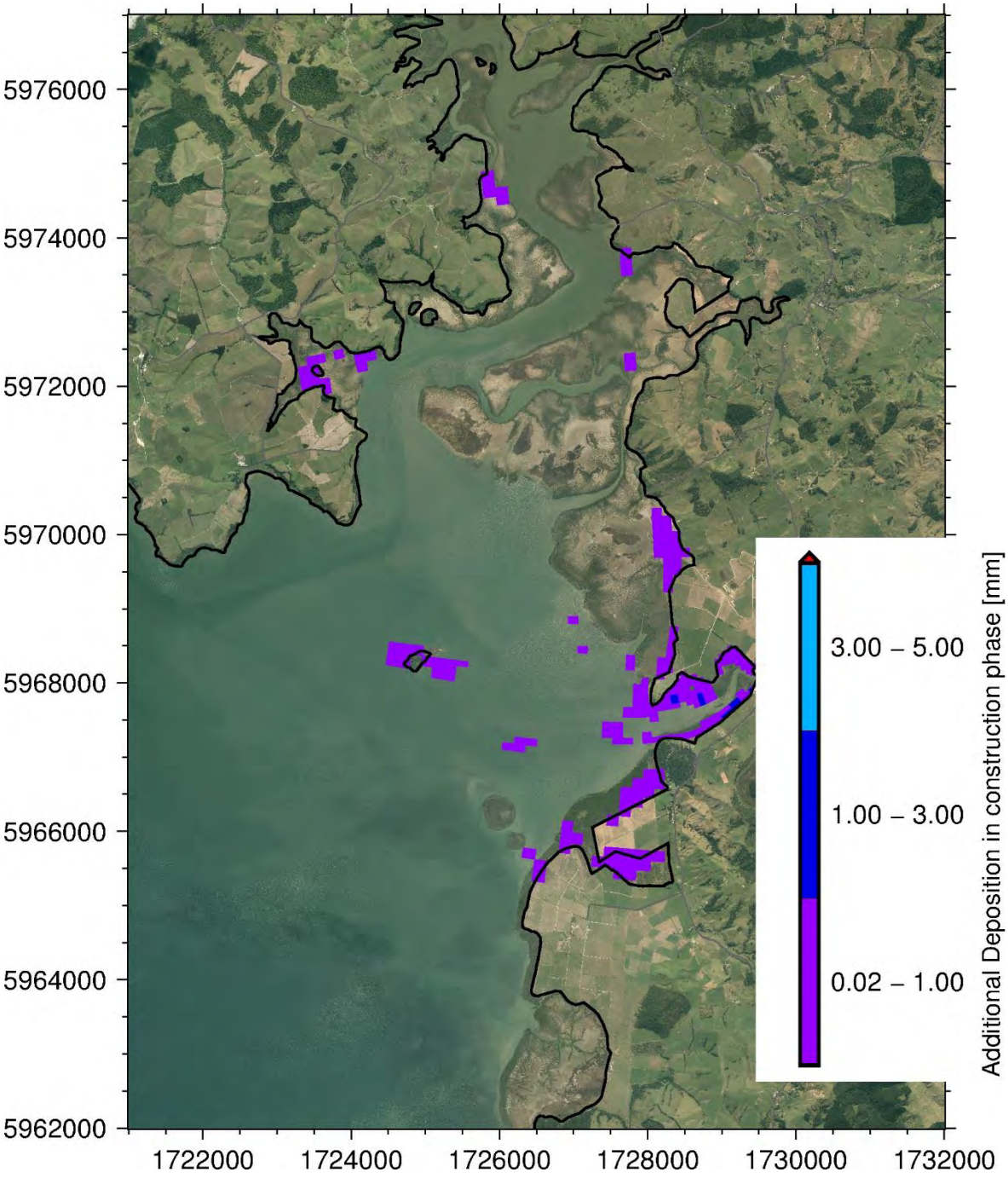

Figure 110: Additional deposition arising from Project construction at 3 days after the start of the event for the 10-year ARI, SW wind event. Note: additional deposition lower than 0.02 mm are not shown here.

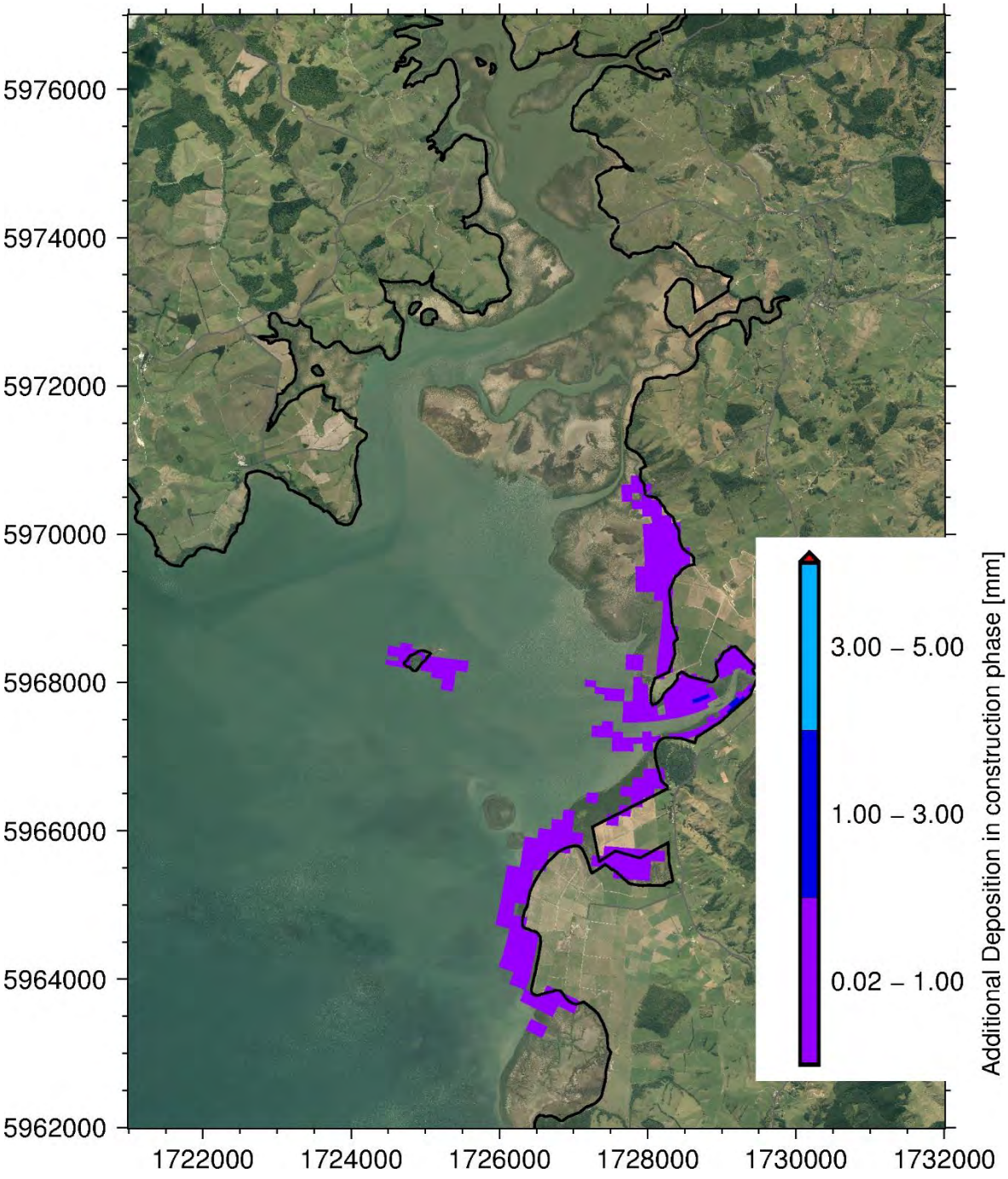

Figure 111: Additional deposition arising from Project construction at 3 days after the start of the event for the 10-year ARI, NE wind event. Note: additional deposition lower than 0.02 mm are not shown here.

Additional deposition arising from Project construction at 3-days after the start of the event for the 50-year ARI events

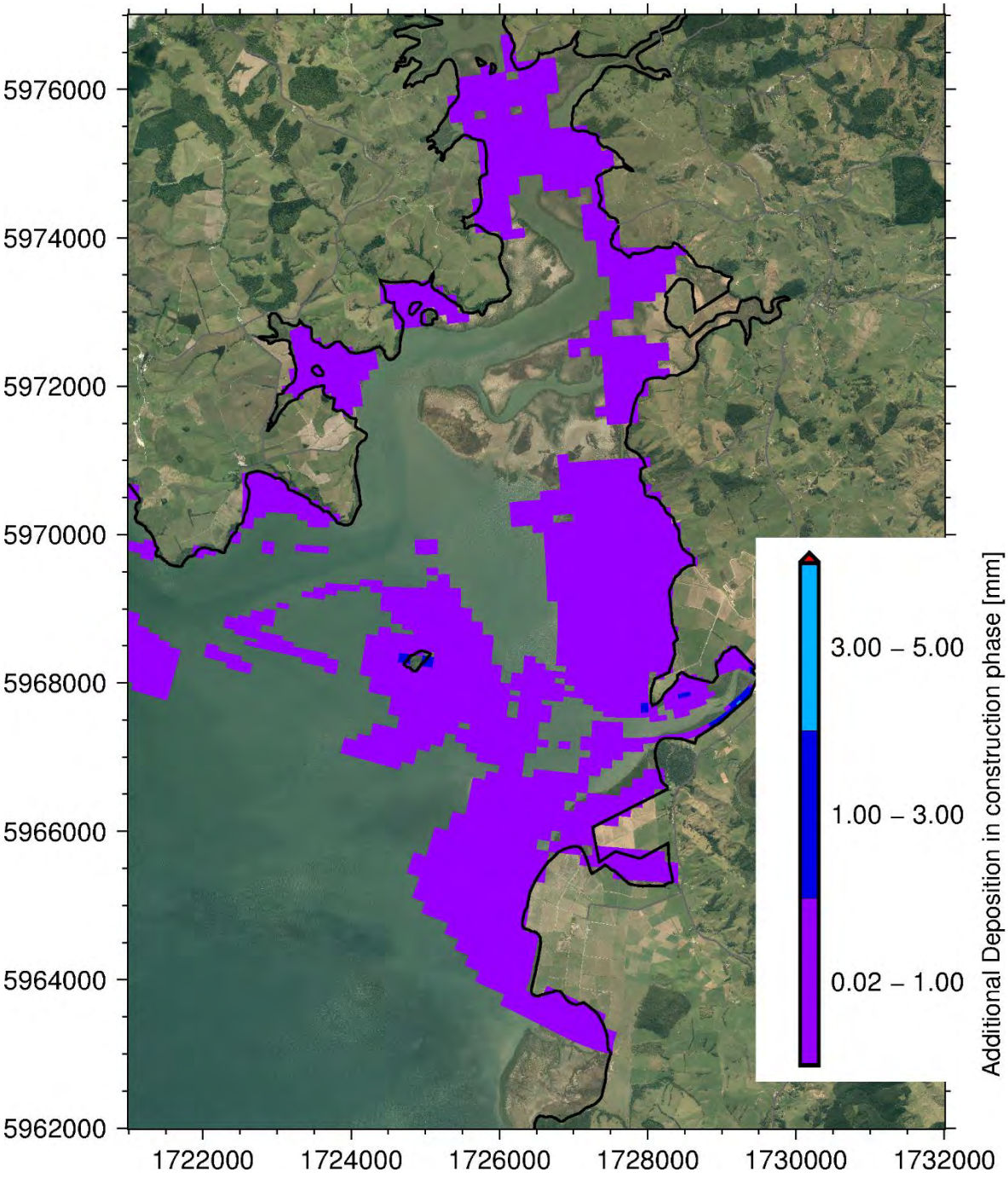

Figure 112: Additional deposition arising from Project construction at 3 days after the start of the event for the 50-year ARI, calm wind event. Note: additional deposition lower than 0.02 mm are not shown here.

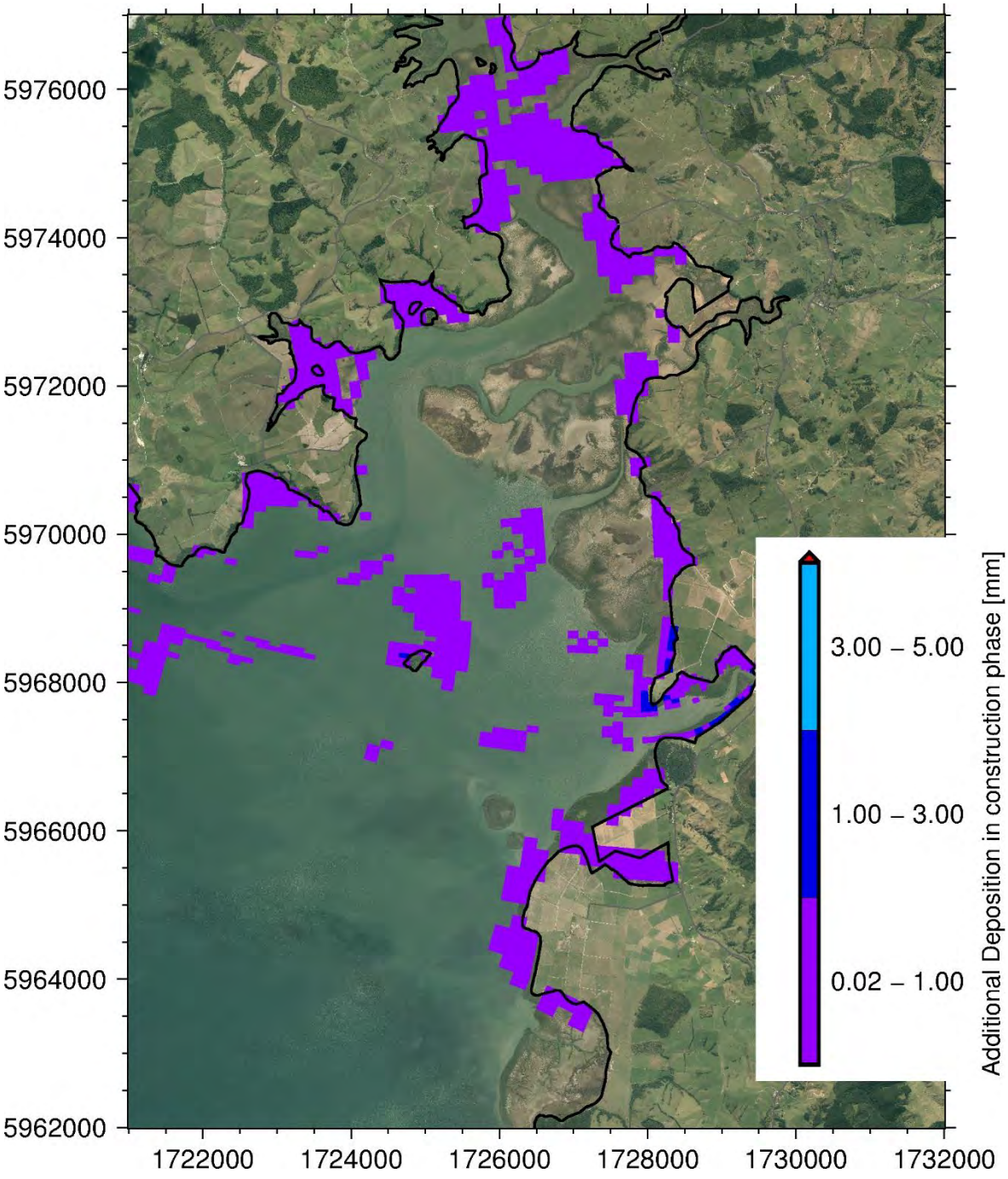

Figure 113: Additional deposition arising from Project construction at 3 days after the start of the event for the 50-year ARI, SW wind event. Note: additional deposition lower than 0.02 mm are not shown here.

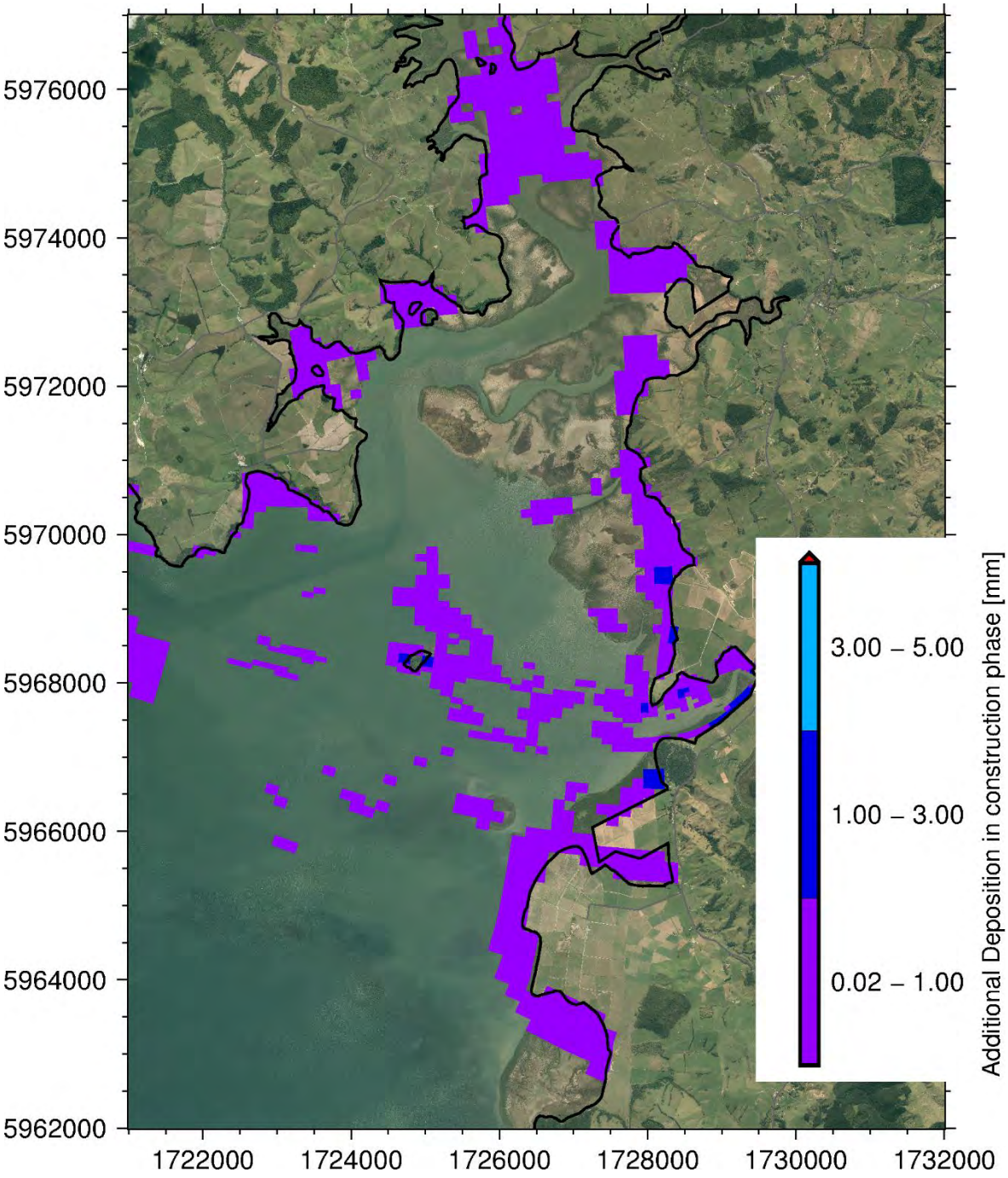

Figure 114: Additional deposition arising from Project construction at 3 days after the start of the event for the 50-year ARI, NE wind event. Note: additional deposition lower than 0.02 mm are not shown here.

Additional deposition from the construction phase at the end of 7-day simulation for the 10-year ARI event

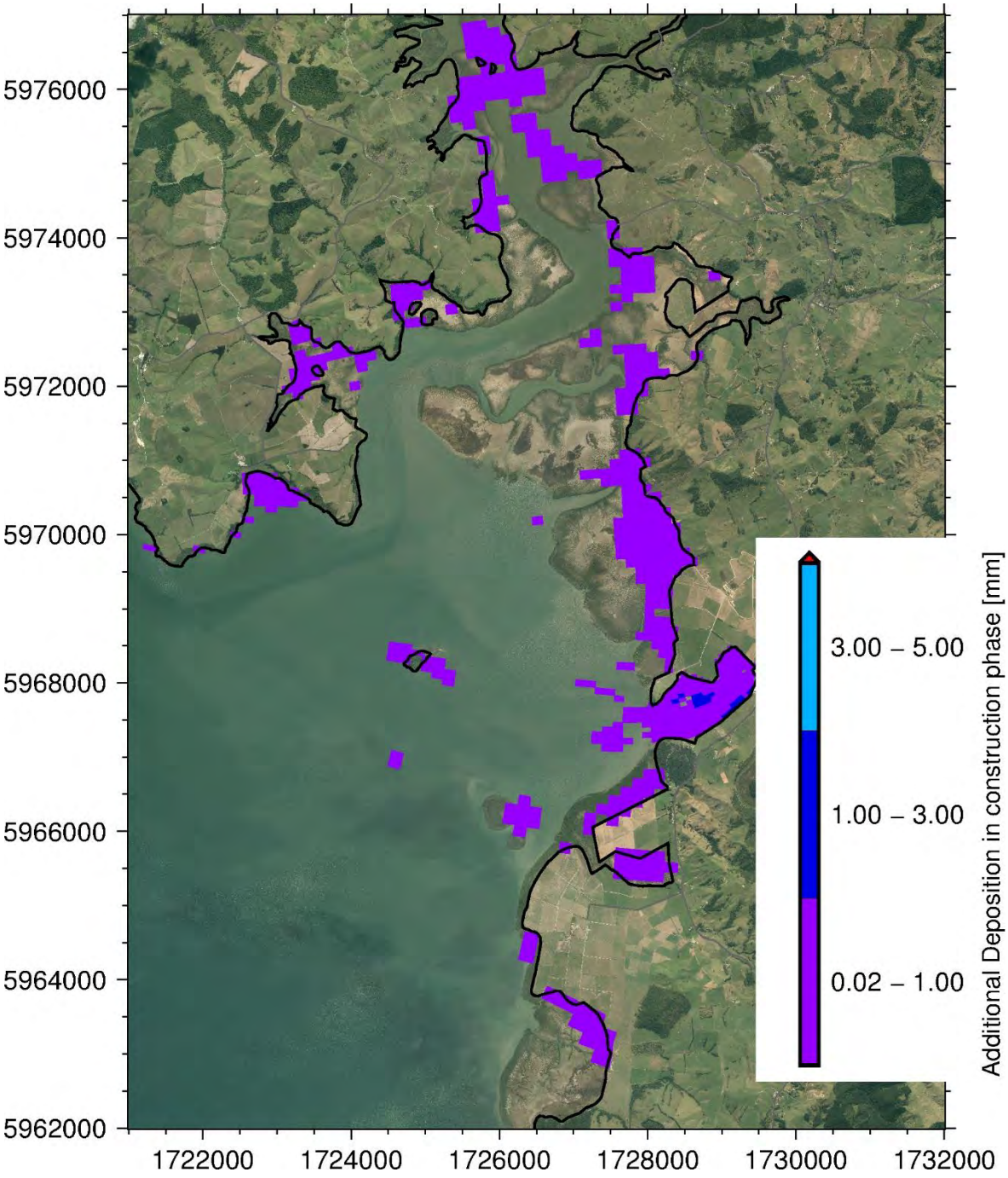

Figure 115: Additional deposition from Project construction at the end of 7-day simulation for the 10-year ARI, calm wind event. Note: additional deposition lower than 0.02 mm are not shown here.

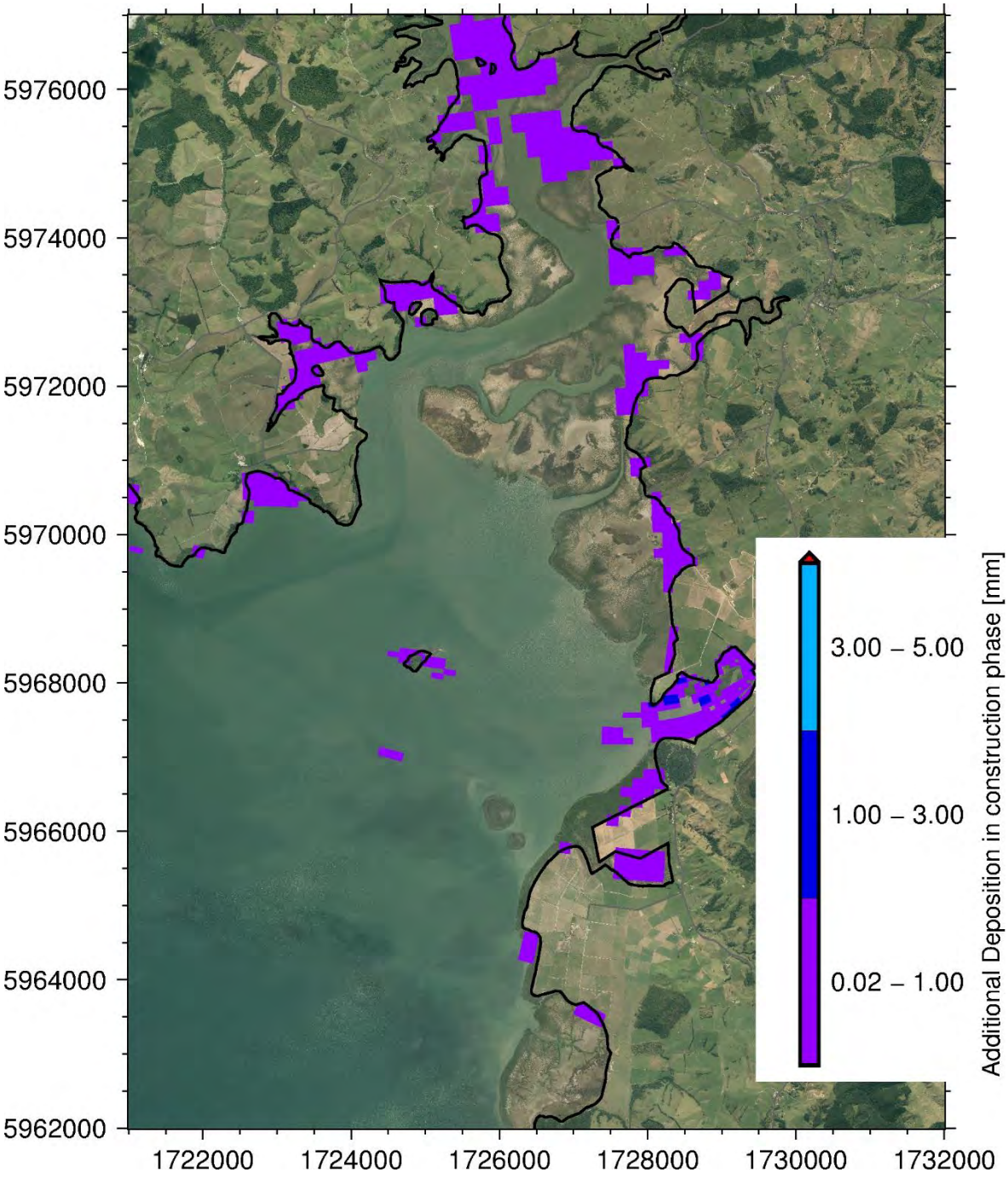

Figure 116: Additional deposition from Project construction at the end of 7-day simulation for the 10-year ARI, SW wind event. Note: additional deposition lower than 0.02 mm are not shown here.

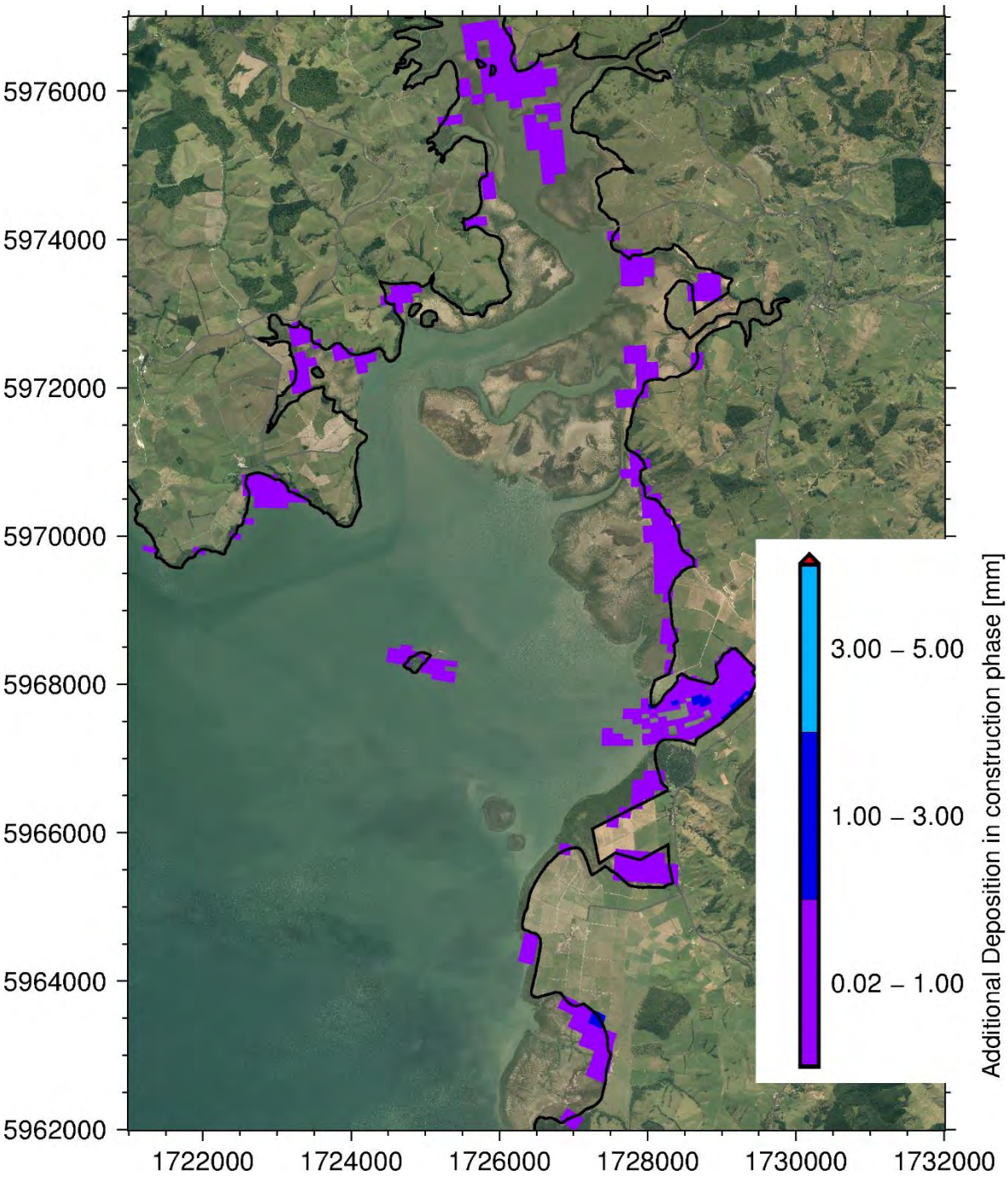

Figure 117: Additional deposition from Project construction at the end of 7-day simulation for the 10-year ARI, NE wind event. Note: additional deposition lower than 0.02 mm are not shown here.

Additional deposition from the construction phase at the end of 7-day simulation for the 50-year ARI event

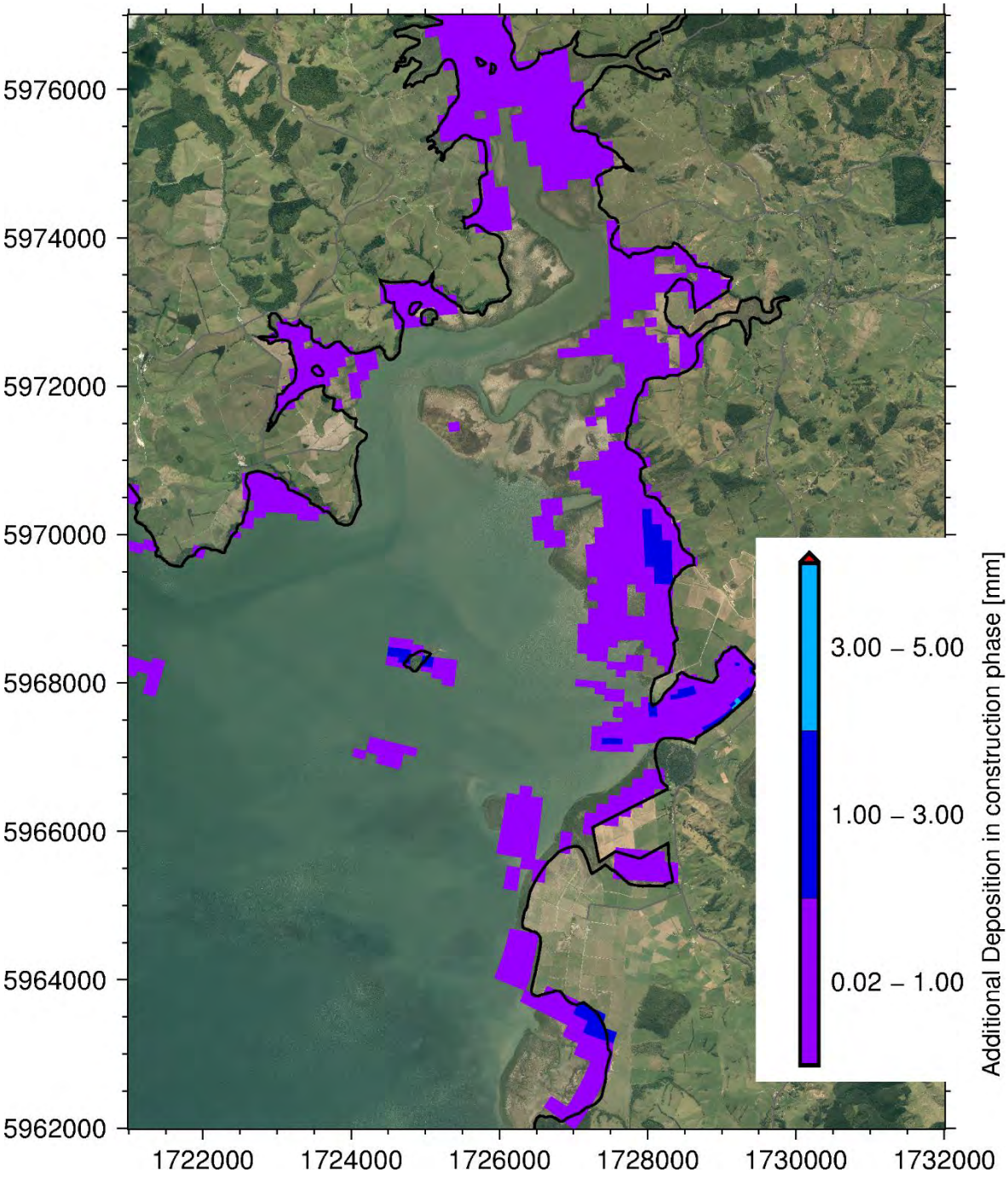

Figure 118: Additional deposition from Project construction at the end of 7-day simulation for the 50-year ARI, calm wind event. Note: additional deposition lower than 0.02 mm are not shown here.

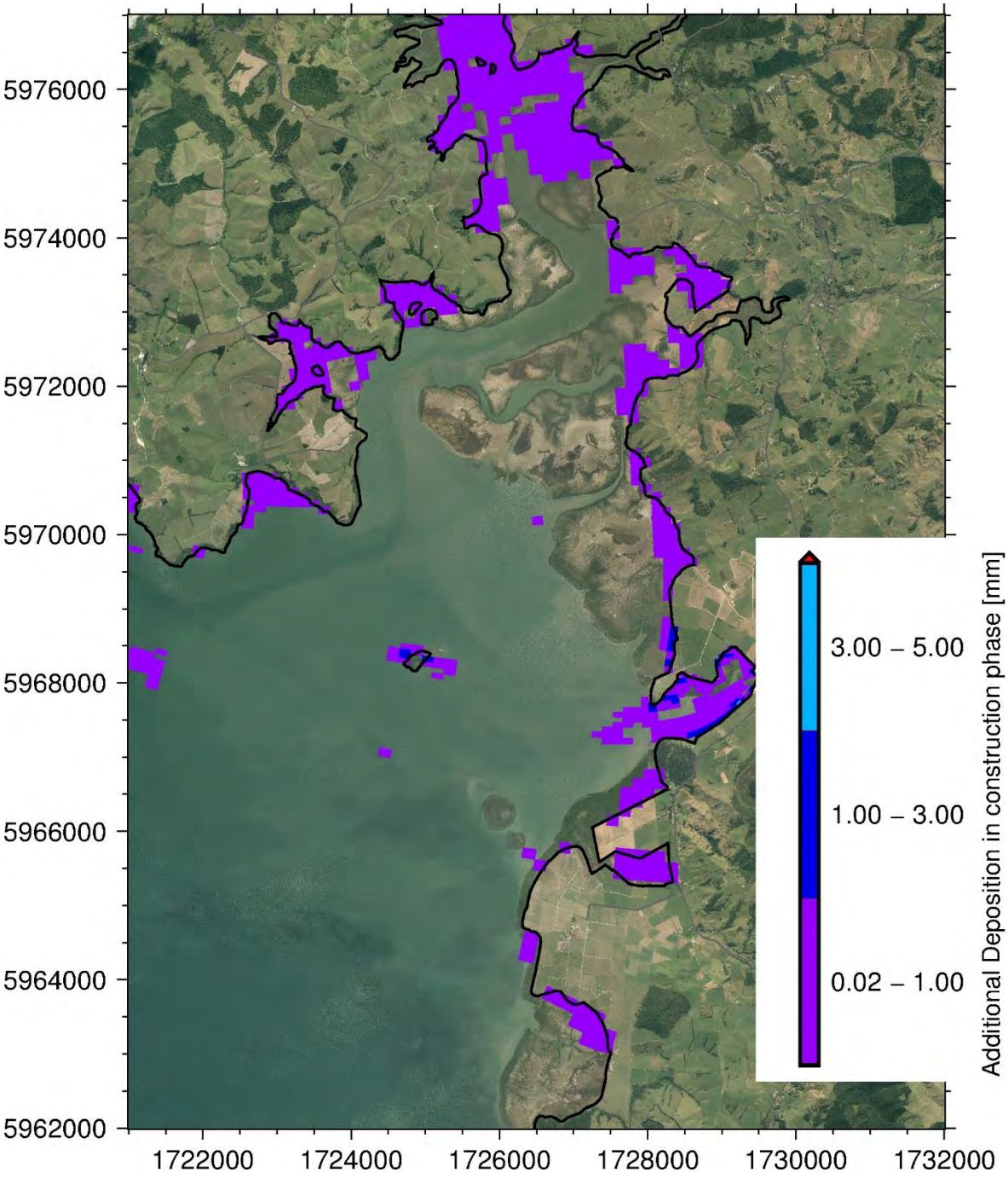

Figure 119: Additional deposition from Project construction at the end of 7-day simulation for the 50-year ARI, SW wind event. Note: additional deposition lower than 0.02 mm are not shown here.

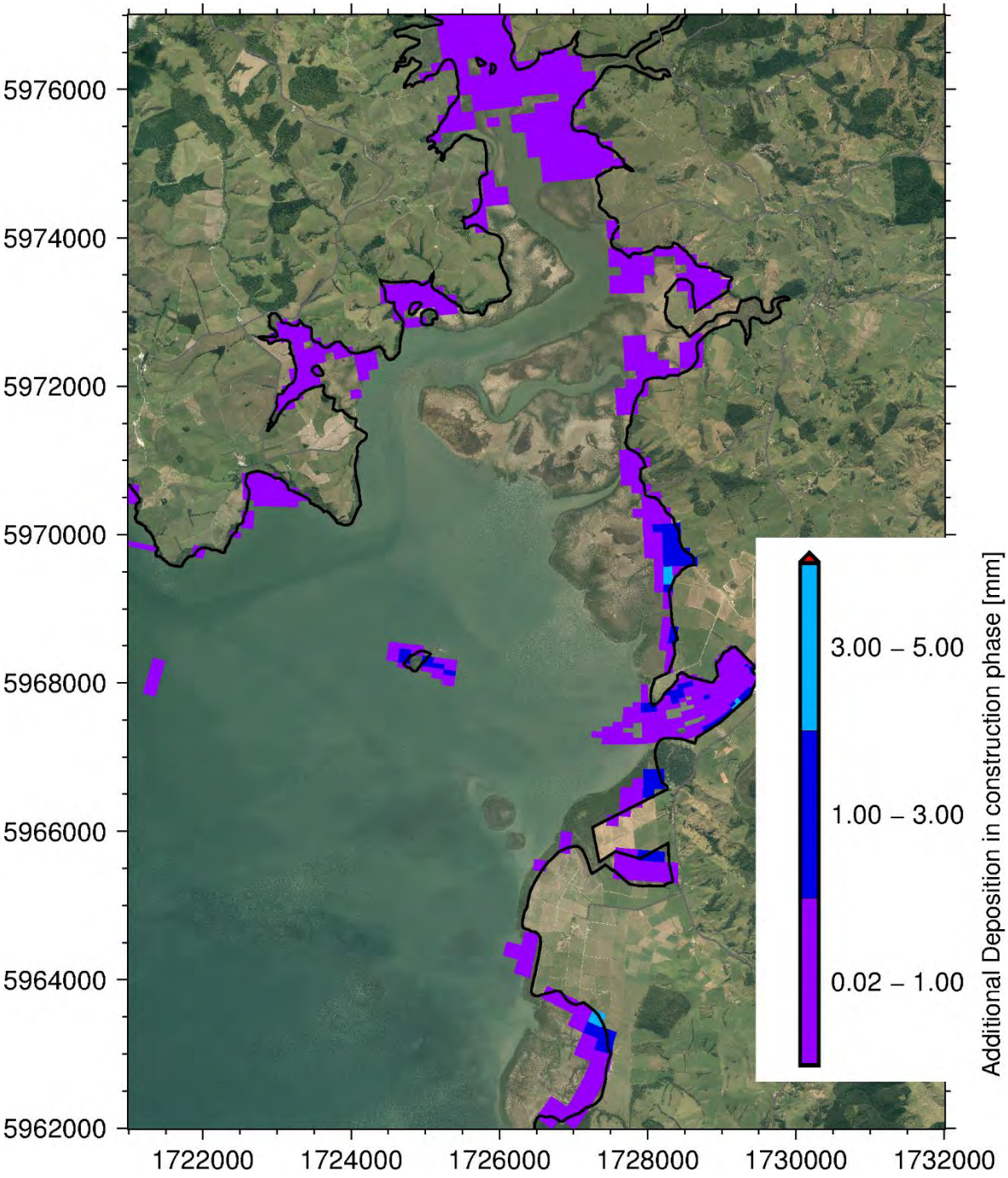

Figure 120: Additional deposition from Project construction at the end of 7-day simulation for the 50-year ARI, NE wind event. Note: additional deposition lower than 0.02 mm are not shown here.

APPENDIX E: ORUAWHARO RIVER SITE VISIT NOTES

Site visit

A vessel-based site visit was undertaken on Friday 16th February 2018. Weather on the day was fine with light northerly winds and no waves. The journey was timed to coincide with high-tide in the upper reaches of the creek arms to allow inspection as far upstream as possible. The predicted high tide was 12:34 pm at Port Albert, with high-tide estimated to be 60 minutes later in the uppermost tidal reaches.

While the weather during the inspection was calm, the weather over week prior to inspection had been wet (approximately 110 mm rain[7]) and windy (typical daily gust speeds > 40 km/hr). Water clarity throughout was poor with visibility estimated to be less than 0.5 m at all times.

Table 20 briefly outlines the site visit timetable. Inspection of the upper reaches was prioritised as the upper estuary is the most sensitive to fine-sediments and has the greatest area of receiving environment.

Table 20: Site visit overview.

Location	Time	Tide stage, flow direction	Comments
Lower Oruawharo River; Hargreaves Basin to Port Albert.	0910 – 1030	Low-mid tide, incoming.	Hargreaves Basin inspection truncated 1.5 km from Gitto's Point due to mechanical issues.
Oruawharo River; Port Albert to Topuni River	1240 – 1248	Mid-high tide, incoming	
Topuni River; 3 km from Oruawharo confluence	1248 – 1259	Mid-high tide, incoming	Short inspection only as no works/discharge planned in this catchment.
Lower Maeneene Creek; below confluence with Te Hana Creek	1300 – 1324	Mid-high tide, slack	
Upper Maeneene Creek; Rail bridge	1341	High tide, slack	
Upper Maeneene Creek; limit of inspection.	1402	High tide, outgoing	Creek too narrow to continue. Within 200 m from existing SH1, highway vehicles audible but not visible.
Te Hana Creek, to existing SH1 and rail bridges	1424 – 1440	Mid-high tide, outgoing	
Te Hana Creek; limit of inspection.	1442	Mid-high tide, outgoing	50 m upstream from existing bridges.
Photographing Ecological monitoring sites	1305	Mid-high-tide, outgoing	

[7] Estimated based on 125 mm at Whangarei Airport and 109 mm at Whangaparaoa AWS. See www.metservice.com

Figure 121: Site location map with named points of interest and vessel path (red). Total journey length 30 km [Image date 6-10-2017, *Source*: Google Earth].

Site description

The observations within the Oruawharo River is presented here sequentially from the downstream end at the outlet to the Otamatea Channel, upstream through to the upper reaches of Maeneene and Te Hana Creeks.

Lower Oruawharo Arm and Hargreaves Basin

Hargreaves Basin and the upper Oruawharo Arm are separated from the body of the Northern Kaipara Harbour by a narrow entrance or throat that is 9 km long and 700 m wide (Figure 122). Water depth along at the throat is typically greater than 10 m, but reaches more than 20 m in localised scour holes and channel constrictions (e.g., Schnapper Point, Motukumara Point – see Figure 122). The throat of this flanked by the hillsides of Oruawharo Heads and Puketotara Peninsula. The fringe of the throat has mangroves colonising the narrow intertidal banks along with any embayed inlets and stream mouths. Flows within the throat have not been recorded, but are anticipated to be strong tidal flows which convey the large tidal volume to the upper Oruawharo River estuary.

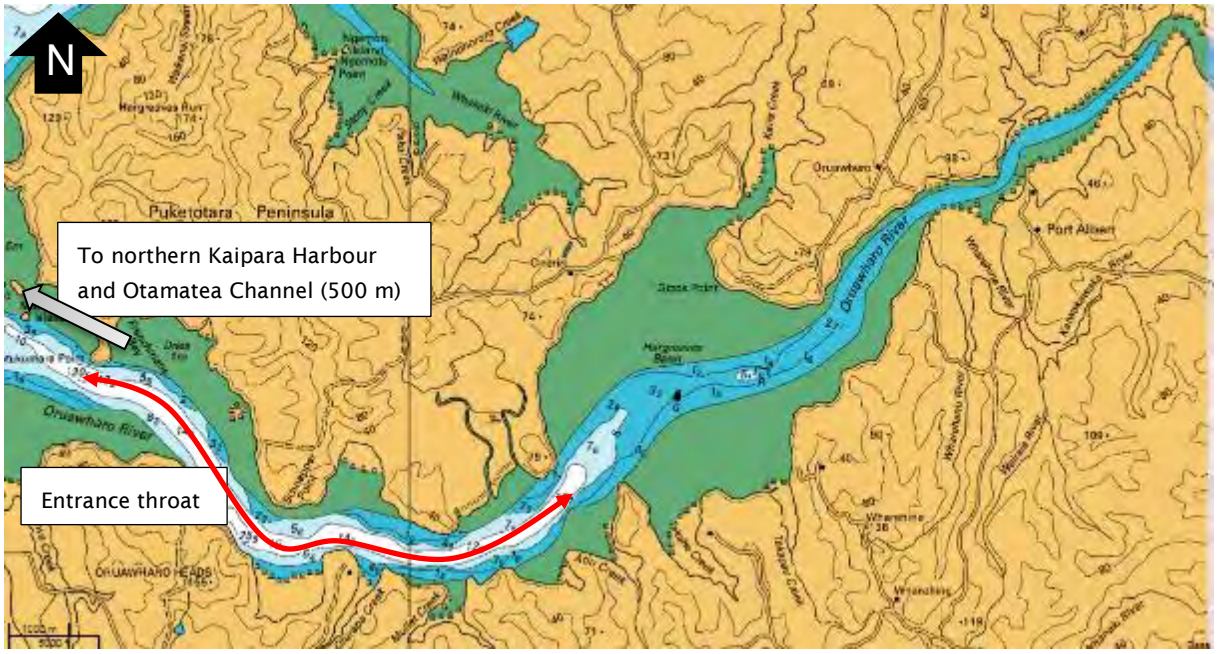

Figure 122: Lower reaches of the Oruawharo River and Hargreaves Basin. North at top. Note limit of map is at right. [*Source*: LINZ chart 4265: Kaipara Harbour].

Hargreaves basin is a roughly circular basin 3 km in diameter (Figure 122) with is northern shores generally sandy/rocky shoreline with eroding hillsides near the water, mangroves occupy most of the southern shoreline and all its tributary streams and sub-estuaries are filled with mangroves. The previously reported areas of salt marsh were not observed due to vessel malfunction (e.g., Hewitt and Funnel, 2004; Swales et al. 2011). The basin is generally shallow and dries to sand-flats and mud-flats at low tide. A central drainage channel bisects the basin from southwest to northwest, grading from 15 m depth in the south to around 2 - 3 m depth in the upper Oruawharo River.

The maximum wave height in Hargreaves basin is likely to be around 0.6 m which may develop at high tide under strong winds from all wind directions. Sediment resuspended by wave action will be advected into sheltered areas such as the mangrove fringe or shallow inlets. The quantity of fine sediments swept downstream into the main body of the Kaipara Harbour will only be small based on previous CSSI sediment tracing (Gibbs et al. 2012) and sediment transport modelling (Green et al. 2017).

Figure 123: Broad expanses of open water in Hargreaves Basin at mid-tide. Photograph viewing north with the tree covered Gitto's Point at right. [*Credit*: M. Allis (NIWA), 16-2-2018 at 0914].

The smaller rivers and streams discharging into the Oruawharo River are generally deeply incised into the intertidal flat, with well-established mangroves (estimated to be at least 30 years old) flanking the outlet channels (Figure 124).

Figure 124: Outflow channels of the Wharehine River (top) and Wharehau Creek (bottom) flanked by well-established mangroves stands. [*Credit*: M. Allis (NIWA), 16-2-2018 at 1024].

Several oyster reefs were observed on the northern shores of the Oruawharo River between Port Albert and Hargreaves Basin (Figure 125). At the time of inspection, a 2 cm coating of fine-sediment was observed on one of the reefs. It is unclear whether the oysters bed contained live oysters. Near the oyster reefs, there is an exposed high-tide beach comprising gravel, shells and sand (Figure 126) indicating high-tide wave-processes. For this beach to form, the oyster beds must have produced and discarded shells in sufficient quantity for waves to mobilise and concentrate at the shoreline. A

small (0.3 m high) wave-created storm berm has formed above the high-water mark and is compose entirely of shell fragments. The berm has isolated a low-lying depression from the main tidal channel and has filled with mangroves (Figure 126). Several other white sandy beaches were observed at the high-tide mark along the northern shoreline (e.g., opposite Port Albert wharf), along with large Macrocarpa trees (approx. 100 years) close to the water.

Figure 125: Oyster reefs outcrops on the northern shoreline of Oruawharo River, near Hargreaves Basin. [*Credit*: M. Allis (NIWA), 16-2-2018 at 0939].

Figure 126: Gravel and shell beach with small storm-berm fronting mangrove filled depression. Oruawharo River, approx. 500m north of Hargreaves Basin [*Credit*: M. Allis (NIWA), 16-2-2018 at 0949].

Central Oruawharo Arm (Hargreaves basin to Topuni River)

Continuing upstream, from Hargreaves Basin to the Topuni River confluence, the flanks of the Oruawharo River are dominated by intertidal flats which are either vegetated with mangroves or remain as unvegetated mudflats. Near Port Albert wharf the southern flats comprise 100 m wide exposed mudflats flanked by a vegetated fringe 10-100 m wide (Figure 127). These exposed flats are very soft mud with occasional oyster beds protruding and a large number of mangrove seedlings which are rapidly colonising the fringe of the mangrove forest and any sheltered intertidal flats. Several mud-thickness measurements were made using a steel rod, with thicknesses greater than 1.5 m observed in many locations throughout this area. Vegetated mud flats appear to fully occupy all inlets excluding small sub-tidal drainage channels which are typically shallow with low current speeds.

Figure 127: Broad intertidal flats immediately west and south of Port Albert wharf. Viewing west as photographed from wharf. [*Credit*: M. Allis (NIWA), 16-2-2018 at 0835].

The main sub-tidal channel of the Oruawharo River was measured at typically 6-9 m deep at mid-high tide (equivalent to 4-7 m Chart Datum) between Port Albert and Topuni River, but was observed (by vessel depth sounder) to reach 16 m depth in a scour depression at the end of the peninsula on which the Port Albert boat ramp and wharf are located. The width of the sub-tidal channel narrows from 120 m near Port Albert to only 80 m near the Topuni River.

Near the confluence of the Topuni River with the Oruawharo River, the intertidal flats appear fully colonised by mangroves with few areas of exposed mudflats. The high-tide channel is flanked by mature mangroves although some dieback of mangroves was observed. No high-tide shelly/sandy beaches were observed through the dense mangrove forest. Several stretches of young mangroves were observed growing in a band 1-3 m wide on the flank of the main channel (Figure 128). This slow expansion and narrowing of the channel is inferred to be from infilling and migration of main channel allowing sediment to deposit and mangroves to colonise.

Figure 128: Slow expansion of intertidal flat shown by new mangrove growth seaward of mature mangroves. [*Credit*: M. Allis (NIWA), 16-2-2018 at 1305].

Maeneenee Creek in the Upper Oruawharo Arm

Maeneene Creek enters the Oruawharo Topuni River 4 km upstream from Port Albert. The entrance is constrained to 150 m wide by a narrowing of the flanking hills, with the hillsides actively eroding due to waves and currents undercutting the bank at high tide. The entrance has 100 m of open water at high tide, with the flanking intertidal flats 50 m wide and colonised by mangroves. Te Hana Creek joins Maeneene Creek 1.8 km upstream from the Oruawharo/Topuni River. The two creeks appear nearly equal in width and flow at their junction.

Alongside Maeneene Creek, large areas with mangrove dieback were observed behind the outer perimeter of healthy and expanding trees. The dead mangrove areas are also occupied by grass/reed stands (Figure 129). Cattle were observed wading/grazing in multiple locations along northern vegetated intertidal flats alongside Maeneene Creek.

Figure 129: Grasses and marsh within mangrove forest, lower Maeneene Creek. Note the few mangrove stumps and dead branches [*Credit*: M. Allis (NIWA), 16-2-2018 at 1321].

Continuing further upstream, the estuary creek continues to narrow between the flanking hillsides. At the rail bridge (4 km upstream, refer Figure 121) the shoreline is 40 m wide, with flanking intertidal flats that are 15 m wide (Figure 130). Mangrove presence is reduced with increased stretches of shoreline covered in pasture grasses.

Figure 130: View upstream in Maeneene Creek at rail bridge, 4 km upstream. [*Credit*: M. Allis (NIWA), 16-2-2018 at 1340].

From 5 to 8 km upstream, Maeneene Creeks flows alongside Waimanu Road to where it meets SH1 (refer Figure 121). In this stretch, the estuary gradually become more riverine in nature. Reflecting this, the proportion of mangroves reduce rapidly with distance upstream and are replaced by pasture grass and trees (see Figure 131).

Figure 131: Absence of mangroves and pasture extending to water level, Maeneene Creek, 7 km upstream. [*Credit*: M. Allis (NIWA), 16-2-2018 at 1351].

At the uppermost limit of the inspection, Maeneene Creek is a narrow channel approximately 4-5 wide between stream banks, and less than 1.5 m deep at high tide (Figure 132). The environment is riverine in nature, and appears beyond the limit of saltwater intrusion.

Figure 132: View upstream at limit of site visit, Maeneene Creek Photograph at approximately 200 m from existing SH1 and junction with Maeneene Road and Waimanu Road. Note absence of mangroves, streambank coverage by grass. [*Credit*: M. Allis (NIWA), 16-2-2018 at 1404].

Te Hana Creek in the Upper Oruawharo Arm

The lower stretches of Te Hana Creek have a lower proportion (compared to Maeneene creek) of areas with mangrove dieback and a smaller areas of intertidal grasses, and the mangroves vegetation also appeared in better overall condition than Maeneene Creek.

The inspection of Te Hana Creek was truncated at the existing state highway bridge due to time limits (Figure 133). At this location, 3 km upstream, the creek remains estuarine dominated, with mangroves stands occupying narrow intertidal flats between the flanking hillsides. Upstream, aerial photos indicate that there are increased stretches of shoreline covered in pasture grasses.

Figure 133: View upstream at limit of site inspection, Te Hana Creek. [*Credit*: M. Allis (NIWA), 16-2-2018 at 1440].